A TIME-DIVISION-MULTIPLEX LASER COMMUNICATIONS SYSTEM

A THESIS

Presented to

The Faculty of the Graduate Division

by

William Taylor Mayo, Jr.

In Partial Fulfillment

of the Requirements for the Degree

Master of Science in Electrical Engineering

Georgia Institute of Technology

June, 1966

A TIME-DIVISION-MULTIPLEX LASER

COMMUNICATIONS SYSTEM

Approved: ______________________

____

____

Date approved by Chairman: 5/12/66

ACKNOWLEDGMENTS

On completion of the work reported herein, I wish to thank Dr. W. B. Jones, Jr., my thesis advisor, for the suggestion of the problem and guidance during all phases of the project. The writing of the thesis benefited greatly from his constructive criticism of the drafts. Special thanks are due to Dr. T. M. White, Jr., who served on the reading committee and provided guidance during the final construction of some of the system components. Thanks are also due to Dr. Eugene Harrison of the Mechanical Engineering Department, who served as the third member of the reading committee and made suggestions for clarification of the final draft. In addition, I wish to thank Dr. B. J. Dasher, Director of the School of Electrical Engineering, and many other members of the Electrical Engineering staff for equipment, parts, and aid in construction details. For fellowship support of my graduate program, I wish to express great appreciation to the National Science Foundation.

TABLE OF CONTENTS

LIST OF ILLUSTRATIONS

LIST OF SYMBOLS

Symbol	Definition	Page
k_i	Coefficient in power series for system transfer function	26
K_1, K_2	Constants relating phase shift to applied voltage in KDP modulator.	3
L	Length of KDP crystal in z direction.	3
N	Index of refraction	2
N_1, N_2	Indices of refraction in medium exhibiting birefringence	2
P	High voltage output power	41
P_{min}	Lower bound on high voltage output power.	42
R	Shunt output resistance	40
t	Off time between samples.	35
U	Energy per pulse in power calculation	41
v	Phase velocity of light in a refractive medium. . . .	2
v_1, v_2	Light component phase velocities in birefringent medium.	3
V	Peak amplitude of audio test signals.	26
V_m	Modulating voltage applied to crystal	3
V_{max}	$= I_{max}R$ = rms. peak pulse modulating voltage.	41
V_Π	Voltage required for $\Delta\psi = 180°$, or "half-wave" voltage	5
V_{in}	Input voltage to final high voltage stage	19
V_{out}	Output voltage of final high voltage stage.	19
w_o	Light frequency (radian).	44
w_s	Modulating frequency (radian)	45
W	Pulse rate.	41

Symbol	Definition	Page
Δf	Frequency separation in multimode laser	45
Δw	$= 2\Pi \Delta f$	46
$\Delta \psi$	Phase shift between light components in electro-optic material.	3
$\Delta \psi_o$	Constant phase shift from birefringent plate.	6

SUMMARY

A time-shared multichannel laser communication system has been designed, constructed, and evaluated. Although the overall system bandwidth would have allowed at least 25 audio channels, only two such channels were implemented. The amplitude sample duration, as well as the time between samples, was nominally 2 μsec. However, both the sample duration and pulse spacing were variable for purposes of evaluation. Sample pulses were multiplexed, amplified to an average value of approximately 1000 volts, and applied to a longitudinal KDP light-intensity modulator. The carrier was a columnated beam from a multimode helium-neon gas laser operated at 6328 Å. The receiver consisted of a photomultiplier detector, a wideband amplifier, demultiplex gating, audio filters, and audio amplifiers.

Evaluation results suggest some of the problems of a practical time-division-multiplexed system. Mechanical vibration of the laser mirrors is one source of undesirable amplitude variation which becomes audible with an amplitude modulation scheme. A possibly more serious problem arises from the piezo-optic effect, that is, modulation due to mechanical crystal strain in the KDP material. Since all electro-optic materials, including KDP, are piezoelectric, the modulating pulse voltages introduce crystal strain and hence piezo-optic modulation. This modulation was found to lead to cross talk in the constructed system.

Modulation power and bandwidth limitations are discussed briefly, treating the modulator as a parallel plate capacitor. It is shown that,

when a multimode laser is used for the carrier source, low-pass, wide-band signals are limited to a bandwidth not greater than one half the separation between the light frequencies.

CHAPTER I

INTRODUCTION

The Problem

The objectives of this research have been the design, construction and evaluation of a multichannel voice communications system employing a coherent light beam carrier. A laser beam was intensity modulated with a time-division-multiplexed signal. Receiving equipment detected, demultiplexed, and demodulated this signal. Although the system was inherently capable of transmitting 25 voice channels, only two adjacent channels were implemented.

Background

Optical Communication

Even though optical communication is as old as the evolution of the eye, the laser has given it a new birth by providing coherent light. This gives the communications engineer an electromagnetic carrier wave whose frequency of 10^{14} cps is orders of magnitude higher than that of microwaves. The two greatest advantages of using such a high frequency carrier are the large theoretical bandwidth possible and the extreme directivity obtainable. Even if the possible bandwidth is not utilized, the directivity property greatly reduces transmitter power requirements as compared with lower frequency systems. However, the directivity may also be a disadvantage in that very critical angular alignment is required.

There are two articles by Otten[1] and Fusca[2] which provide a good introduction to laser communications. Fusca shows that for an interplanetary communications system limited to 100 pounds in weight, a laser system would offer a one-hundred-fold increase in data rate or a ten-fold increase in range over a more conventional microwave system.

Optical Amplitude Modulation

The linear electro-optic effect, by which the phase properties of light may be altered and which is also known as the Pockel's effect, has been found to be useful for light modulation. Potassium dihydrogen phosphate, or KDP, is a clear crystalline material which exhibits the Pockel's effect. It has been widely used for light intensity modulation and is now available commerically, cut, polished and mounted with electrodes for this purpose. A KDP modulator crystal was used for this research.

A material is said to be birefringent if its dielectric constant, and hence its index of refraction, is a function of the polarization of an electromagnetic wave passing through it. Calcite and KDP are two examples of crystals which are naturally birefringent at optical wavelengths. A light beam passing through one of these crystals is decomposed into two linearly polarized beams whose E-field vectors are perpendicular to each other and the direction of the beam. These two linearly polarized components are oriented with respect to the crystal in such a manner that the index of refraction is different for one component than for the other. Let these two indices of refraction be designated N_1 and N_2.

The phase velocity of light in a medium is given by

$$v = \frac{c}{N} \tag{1}$$

where c is the free space velocity of light and N is the index of refraction. Thus the two linearly polarized components of light emerging from a birefringent crystal have traversed the crystal at different velocities:

$$v_1 = \frac{c}{N_1} , \qquad v_2 = \frac{c}{N_2} . \tag{2}$$

The difference of these velocities may be expressed for a specific orientation and thickness of the crystal as some phase shift, $\Delta\psi$, of the two components with respect to each other.

Although KDP is a naturally birefringent crystal, the effect is not present for light traveling parallel to the optic axis of the crystal. However, if an electric field is applied, also parallel to the optic axis, the crystal becomes birefringent in this direction, and the phase shift is linearly proportional to the applied field strength and the length of the crystal. This longitudinal, electrically-induced birefringence is a specific example of the Pockel's effect. The importance of transverse effects, which also exist for some materials, will be discussed later.

If the required electric field, E_m, is applied by flat surface electrodes with small holes for the light beam, as illustrated in Figure 1, the resulting field will be proportional to the applied voltage, V_m, divided by the length of the crystal, L. The phase shift produced is

$$\Delta\psi = K_1 E_m L = K_1 K_2 \frac{V_m}{L} L = K_1 K_2 V_m \tag{3}$$

where K_1 and K_2 are constants of the material and the electrode configuration respectively. K_1 is actually a function of the wavelength of the

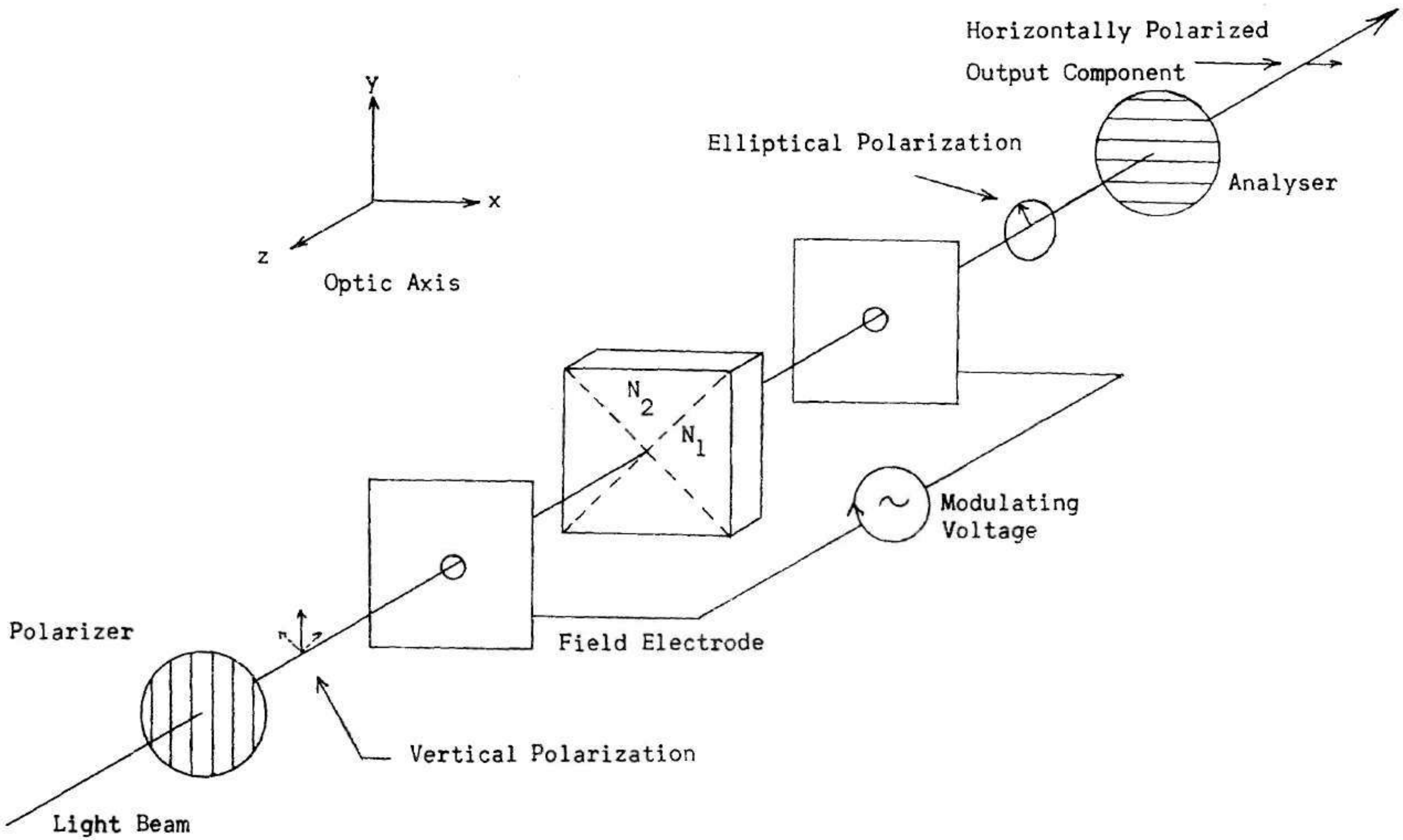

Figure 1. Exploded View of KDP Crystal Modulator.

light, but for a monochromatic source such as a laser, it is constant. Phase shift of 180° may be obtained if the applied voltage is equal to V_Π, a constant which depends on K_1 and K_2. This "half-wave" voltage is greater than 7500 volts in the case of KDP. The phase shift may thus be expressed as

$$\Delta\psi = \Pi \frac{V_m}{V_\Pi} . \tag{4}$$

An optical amplitude modulator may be constructed by placing a KDP crystal, with electrodes as described above, between two polarizers. The polarizers are first aligned in perpendicular directions, as shown in Figure 1, so that the light beam is not transmitted. The KDP crystal is then oriented with its optic axis parallel to the beam and with the two perpendicular polarization axes 45° with respect to the polarizers. The linearly polarized beam entering the crystal is decomposed into two equal components along the birefringent axes of N_1 and N_2. Upon exiting the crystal, the components recombine, but due to the phase shift $\Delta\psi$ the beam is elliptically polarized. A component then exists which will pass through the output polarizer, or analyzer as it is called.

It may be shown that the normalized amplitude of the electric field intensity, E_o, of the output light component is given by[3]

$$E_o = \sin \left(\frac{\Pi}{2} \frac{V_m}{V_\Pi}\right) . \tag{5}$$

If the modulated output beam is detected with a square-law photodetector, the detector output current is proportional to the light intensity, that is, the square of the electric field intensity. Then the normalized detector current, I, will be

$$I = \sin^2\left(\frac{\Pi}{2} \frac{V_m}{V_\Pi} \right) . \tag{6}$$

This response, shown in Figure 2, is obviously nonlinear. The linearity of the Pockel's effect refers to the fact that the phase shift, $\Delta\psi$, is a linear function of the applied voltage.

Essentially linear intensity modulation may be obtained for modulating voltages small compared to V_Π if the crystal is electrically biased with a voltage $\pm \frac{V}{2} \Pi$. However, a much simpler non-electrical method of biasing is available. A plate of naturally birefringent material cut to a thickness which gives a phase shift

$$\Delta\psi_o = \pm \frac{\Pi}{2} \tag{7}$$

is called a quarter-wave retardation plate. Such a quarter-wave plate may be placed in the modulator in front of the KDP crystal. Doing so moves the zero signal response point to one of the linear parts of the response curve shown in Figure 2. Then the detector current is given by

$$I = \sin^2\left(\frac{\Pi}{2} \frac{V_m}{V_\Pi} \pm \frac{\Pi}{4} \right) \tag{8}$$

where the sign depends on the orientation of the plate.

In the above discussion no explicit mention of time variation of the variables E_m, V_m, or $\Delta\psi$ has been made. In fact, the above analysis is based on steady-state values for these variables. It has been shown, however, that the relation between $\Delta\psi$ and E_m, given in equation (3), is little affected by time variation of E_m from zero up through microwave

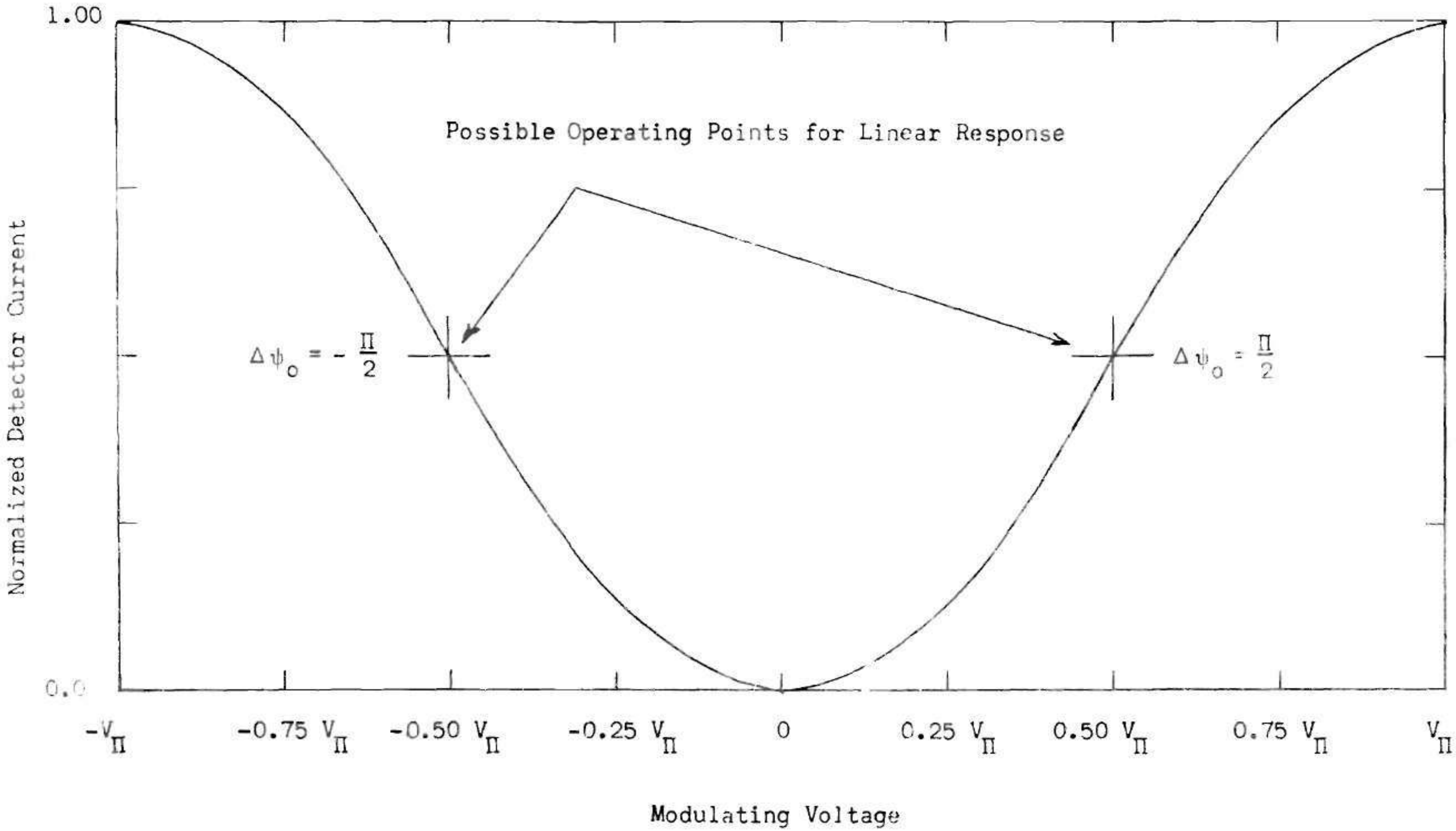

Figure 2. Normalized Detector Current I Vs. Light Modulating Voltage Vm.

rates[3]. Thus KDP modulators are capable of considerable bandwidth. For further reading about electro-optic light modulators, several references are given.[3,4,5,6]

TDM-PAM

Pulse amplitude modulation, or PAM, is obtained by replacing the waveform to be transmitted with a set of uniformly spaced samples of this waveform. Mathematically a PAM waveform is the product of a periodic gating function and the original waveform. If the original waveform has a DC component, the sampled output in the absence of AC components will simply be a uniform pulse train whose amplitude will be called the pedestal. The sampling theorem of communications theory states that if the signal to be sampled may be represented by Fourier components no higher in frequency than f_h, then a sampling rate

$$f_s = 2f_h \tag{8}$$

is sufficient for the original signal to be recovered exactly by use of an ideal low-pass filter. In practice ideal filters do not exist. Sharp cut-off low-pass filters must be used both to limit the highest frequencies of the input signal before sampling and to recover the signal from the sampled waveform. To avoid distortion resulting from the use of non-ideal filters, it is necessary to choose the sampling frequency somewhat larger than twice the nominal cut-off frequency of the input filter.[7,8]

Transmission of a sampled waveform requires greater bandwidth than is required to transmit the same information in unsampled form. However, since there is time between samples which is unused, it is possible to time-division-multiplex, or TDM, the PAM signals and thus send several different signals over the same transmission link. A TDM-PAM waveform is illustrated in Figure 3.

For a telemetry system in which many slowly varying signals are to be transmitted, the entire TDM-PAM process might consist simply of a commutator sweeping around a set of contacts. The signal thus generated could then be used to amplitude modulate a high frequency carrier. At the receiver the amplitude modulated carrier would be detected, and the resulting TDM-PAM signal would be applied to another commutator operating in synchronism with the first. At each contact a PAM signal would appear, which after filtering would represent one of the original signals being transmitted. This example is almost exactly analogous to the proposed system with the radio-frequency carrier replaced by a light beam carrier and the mechanical commutator by an electronic commutator. The only basic difference is that in the light system it is the square of the carrier amplitude which is modulated, rather than the amplitude itself.

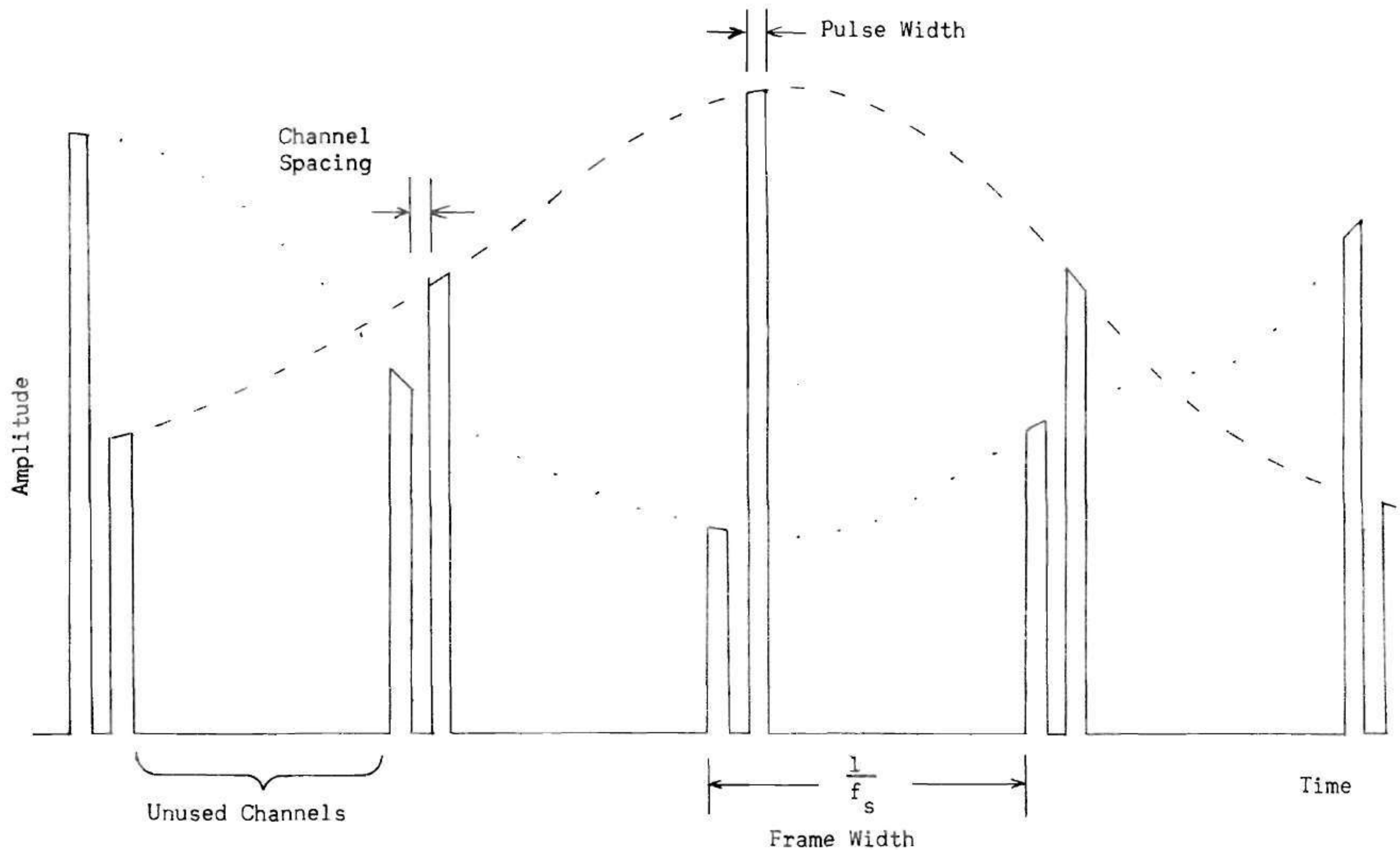

Figure 3. A TDM PAM Waveform Showing Only Two Channels.

CHAPTER II

SYSTEM DESIGN AND CONSTRUCTION

General Considerations

A block diagram of the completed system is shown in Figure 4. As was noted in Chapter I, input filtering, sampling and multiplexing, demultiplexing, and output filtering are essential functions in any TDM voice system. The additional functions shown require some further comment.

In a TDM system the receiver must produce control pulses which sequentially open the gates that separate the multiplexed signal into the individual channel pulse trains. It is generally required that some aspect of the transmitted signal provide a means for the receiver to obtain and maintain gate control synchronization. The arrow labled "Gate Control" in the block diagram indicates that in the laboratory system the demultiplex gate control pulses were transmitted directly by wire. This simplification was made to reduce the required amount of circuit construction, but it did not significantly affect the results obtained.

A KDP crystal modulator employing longitudinal modulating fields requires modulating voltages greater than 1000 volts to effectively utilize the linear part of the system response curve shown in Figure 2. Thus while it was possible to use high speed transistors in the multiplex unit, high voltage vacuum tubes were required for amplification prior to modulation. The high voltage and wide bandwidth requirement of this amplifier will be seen later to be one of the limiting factors of this system.

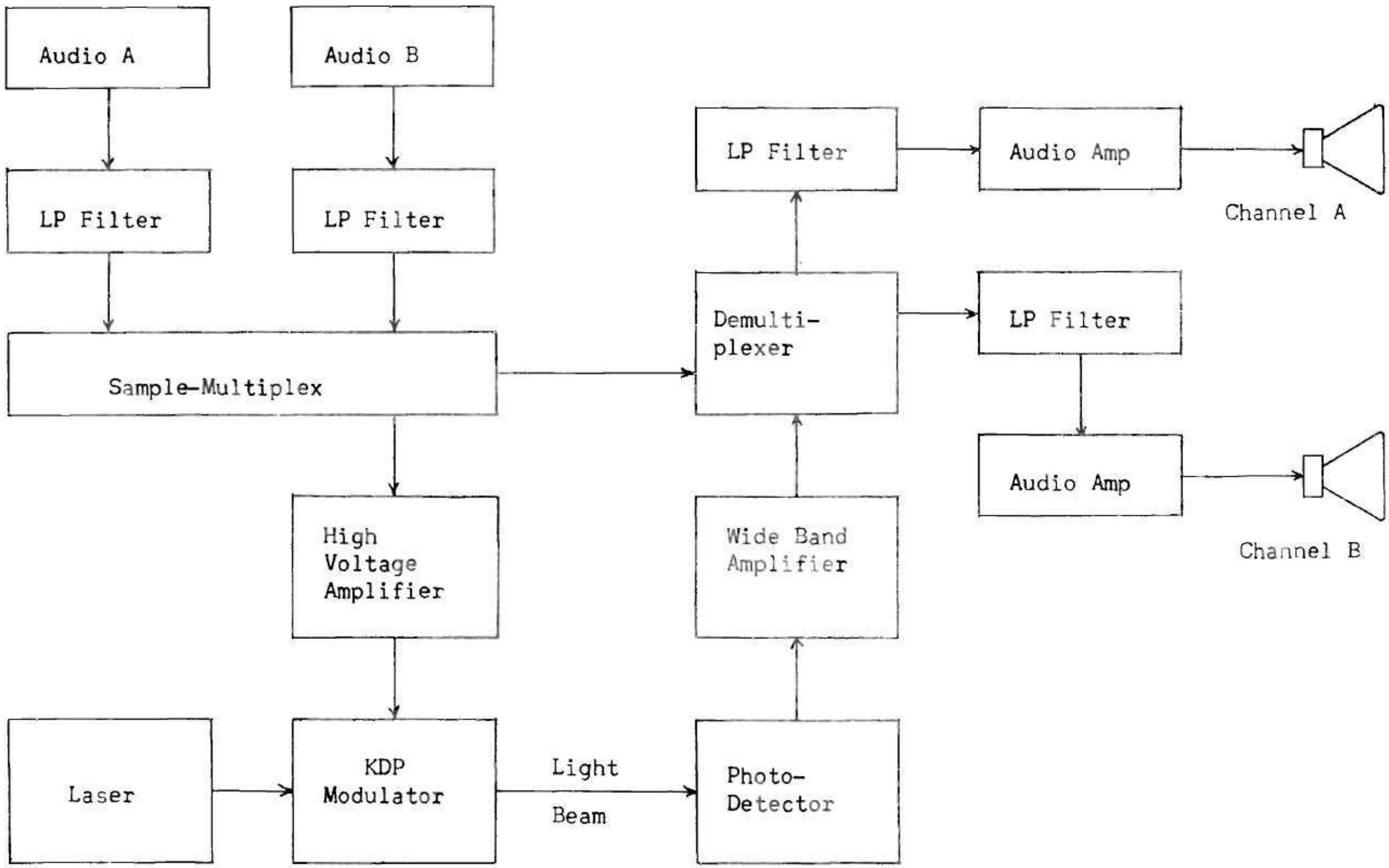

Figure 4. System Block Diagram.

The photodetector shown in Figure 4 is a photomultiplier tube. This device behaves both as an antenna and a square-law detector of visible electromagnetic waves. It acts almost like an ideal controlled current source which responds linearly to the square of the received electric field strength. The photodetector is followed by a transistorized wide-band amplifier which also acts as an impedance matching device for the demultiplex gate circuits.

System Components

The Laser

The coherent light beam necessary for the system was provided by a helium-neon gas laser employing external spherical mirrors spaced 143 cm. apart. The power output of this laser was approximately 0.1 mw at a wavelength of 6328 Å. The mirrors were aligned so that only a single transverse mode set was excited. The output pattern was a (0,0) configuration, that is, a single spot. Excitation was provided by a radio transmitter producing about 40 watts of radio-frequency power at 28 mc. The laser was crudely shock mounted by placing the laser optical bench assembly on a heavy wooden table supported by one-inch thick rubber pads.

The laser and its associated transmitter were not electromagnetically shielded, and due to the wide-band nature of the other equipment being used, problems were incurred from 28 mc interference. These problems were overcome in the following way. The light modulation and demodulation system was placed about 15 feet from the laser on a copper ground screen with all low frequency leads by-passed to it with small value capacitors. Shielded leads and coaxial cables were used where necessary, and a 28 mc blocking filter was built into the input of the receiver wide-band amplifier.

The Multiplex Chassis

Western Electric no. D166019 filters were used as input filters to limit the bandwidth of the audio input signals. A frequency response curve of one of these filters is given in Figure 5. This response was obtained with a 600 ohm audio-oscillator source and a 39 K-ohm filter load resistance. Data was taken with a Tektronix 545B oscilloscope.

The evaluation objectives required a two channel system in which sample duration, channel separation, and sample rate were all variable. No provision was necessary for coding of synchronization signals. System planning indicated that a more efficient high-voltage amplifier could be built if the multiplexed pulses were unidirectional with amplitude variation about the pedestal level of approximately ± 25 per cent.

The block diagram in Figure 6 illustrates functionally how these goals were accomplished. The sample rate was provided by an external audio oscillator. This sinusoidal input was converted to a square wave of the same period by a two state transistor circuit, generally known as a Schmitt trigger. A monostable multivibrator, whose output pulse duration could be varied externally, was triggered each sample period by the negative-going edge of the square wave. The gate control pulses for the two sequential channels could then be taken from two more monostable multivibrators. These were triggered separately by the leading and trailing edges of the output pulse from the first monostable multivibrator. Channel spacing and sample duration could thus be controlled by changing the timing capacitance in the three monostable multivibrator circuits. Provision was made for adjusting the pedestal amplitude of the gated audio signals by leaving the transistor gate bias variable. The sampled

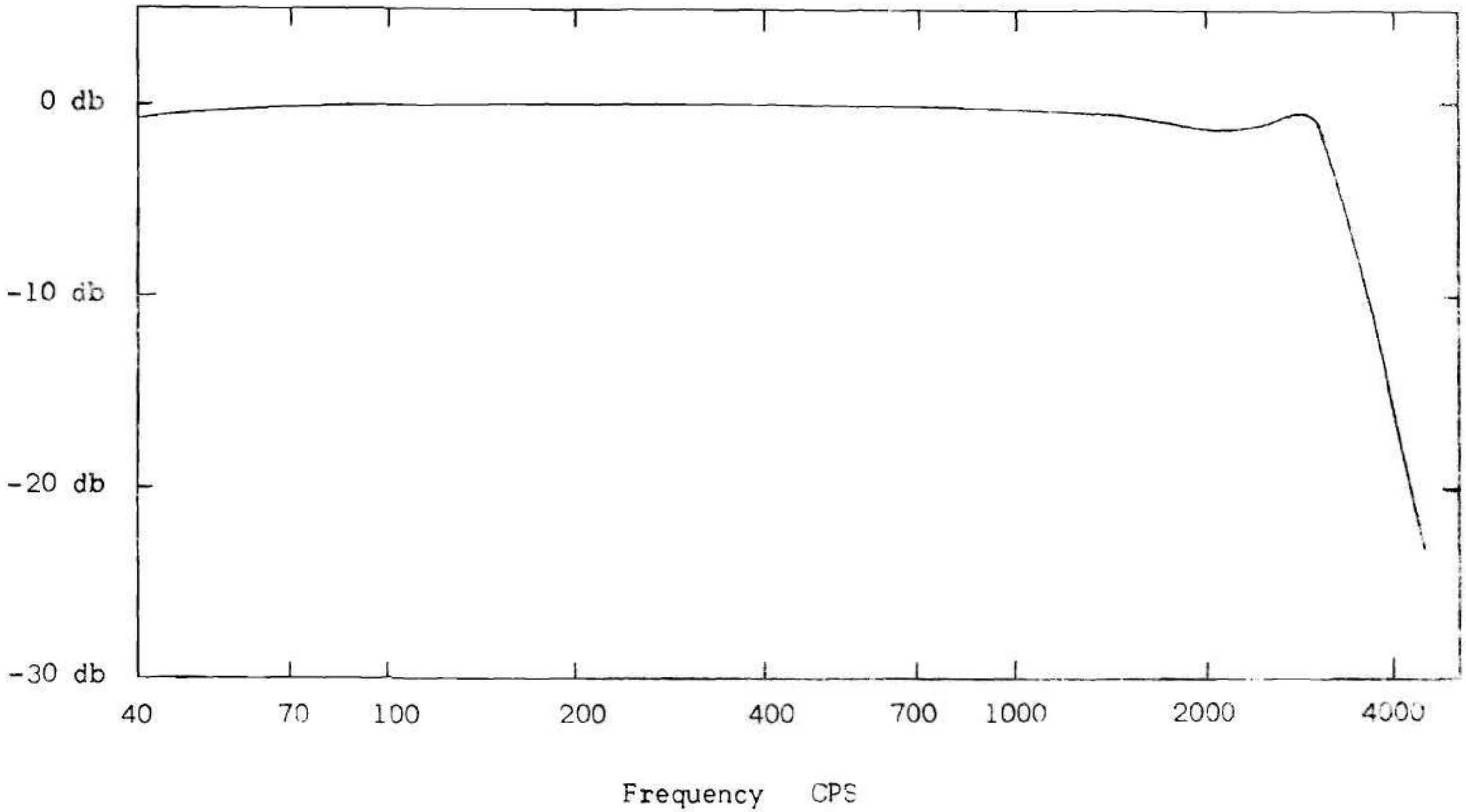

Figure 5. Frequency Response of Western Electric No. D166019 Filter.

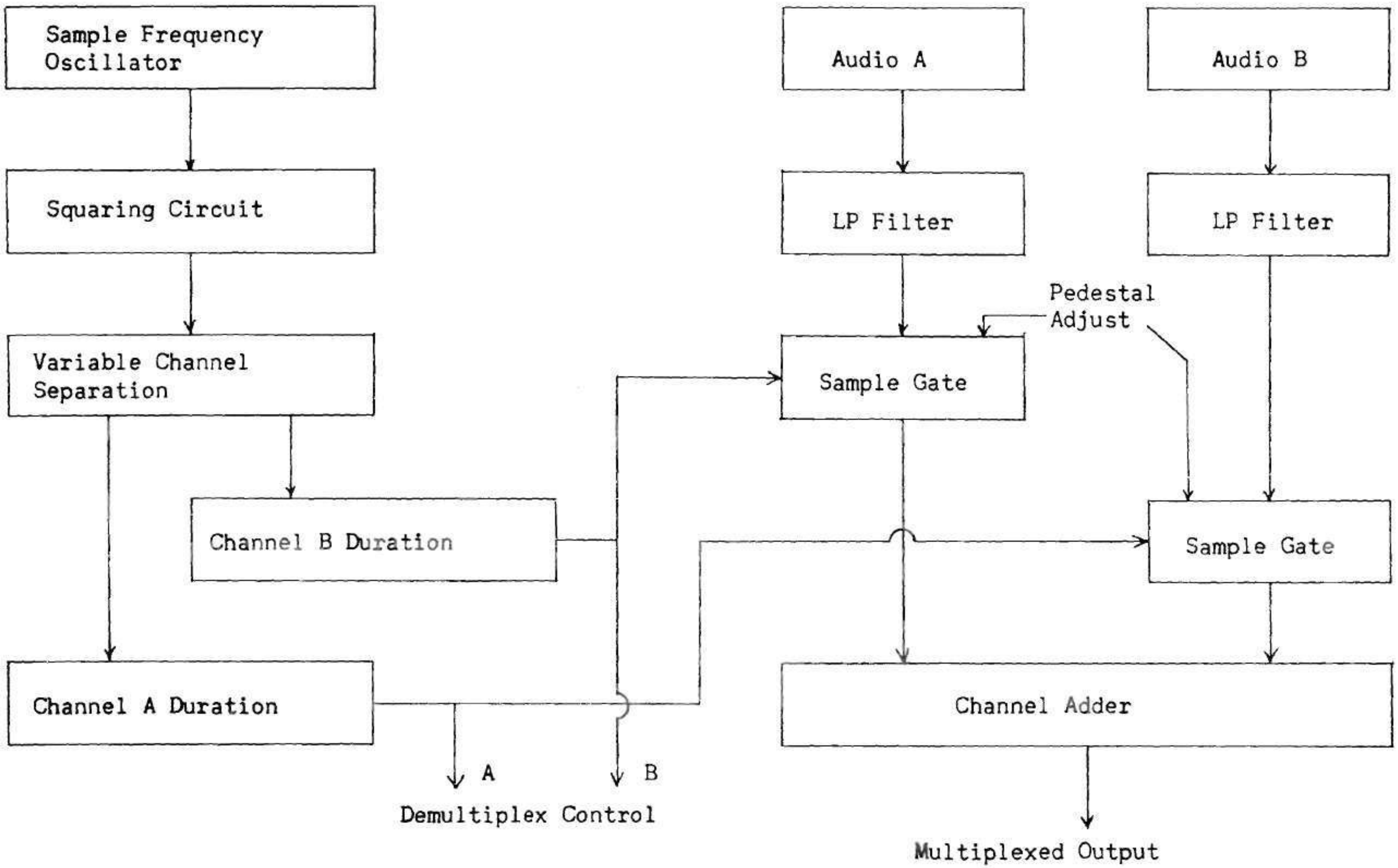

Figure 6. Block Diagram of the Sample Multiplex Unit.

signals were combined in a diode adder to give the multiplexed output. This output consisted, under full input signals conditions, of positive going pulses whose amplitudes were modulated between three and five volts. A schematic diagram of the constructed unit appears in the appendix.

The nominal value chosen for the sample frequency, f_s, was 10 Kc, which implies that the frame width was 100 μsec. Both the sample pulse duration and the off-time between pulses were chosen as 2 μsec. Thus, of the 100 μsec frame width, only 8 μsec were required for two channels and 92 μsec were left. In principle this means that the system had capacity for 23 more identical channels. In all succeeding discussions "channel A" will refer to the first pulse of each frame, and "channel B" will refer to the second pulse.

The KDP Modulator

The KDP modulator chosen for the system was a Baird-Atomic EOLM model JX-1. This modulator consists of a 1 in x 1 in x 1/2 in Z-cut KDP crystal with bonded electrodes. The crystal, electrodes, and glass cover plates are mounted in a teflon case. Two polarizers of the Polaroid type were furnished also, but without specifications concerning them. A retardation plate with phase shift of approximately a quarter-wavelength was used for biasing.

The half-wave voltage, V_π, of the JX-1 at 6328 Å is 10,400 volts. Figure 2 shows that effective use of the linear portion of the response curve would require modulating voltage swings of several thousand volts, with the exact amount depending on the tolerable nonlinearity. Based on restrictions due to the high voltage amplifier, it was decided to use modulating pulse variations of about 1500 volts maximum.

Several properties and restrictions of the JX-1 were important in its use. For frequencies up to a few megacycles, the modulator appears electrically as a 15 μμfd capacitor whose losses are negligible. The crystal is piezo-electric and has a fundamental mechanical vibration resonance which was measured to occur at 35 Kc. It is a property of KDP that mechanical stress from the piezo-electric vibration may cause undesired modulation effects. These and other details concerning the JX-1 may be found in the Baird-Atomic EOLM manual.[9]

The High-Voltage Amplifier

The high-voltage requirements of this amplifier led to the use of vacuum tubes instead of transistors as the most direct approach for the design. Polarity and linearity requirements dictated that the amplifier have two stages of class A_1 amplification prior to the final high-voltage stage. These first two stages were based on a 12AT7 triode followed by a 6L6 pentode, with wide-band characteristics and linearity being obtained by using cathode degeneration and low plate resistance with shunt peaking.[10] The output of the first two stages, when a maximum system input signal was present, consisted of pulses whose amplitude varied from 90 to 150 volts.

The nature of the drive pulses allowed the use of an efficient final amplifier stage biased far into the cut-off region at -150 volts. Figure 7 illustrates how the pedestal of the drive pulses served to bring the stage out of cut-off and place it in the linear region to amplify the variation contained in the upper two-fifths of the pulses. To accomodate the 1500 volt output variation desired, this final stage was implemented with an 813 beam-power pentode, again with shunt peaking.

In that the load seen by this amplifier was a nearly lossless

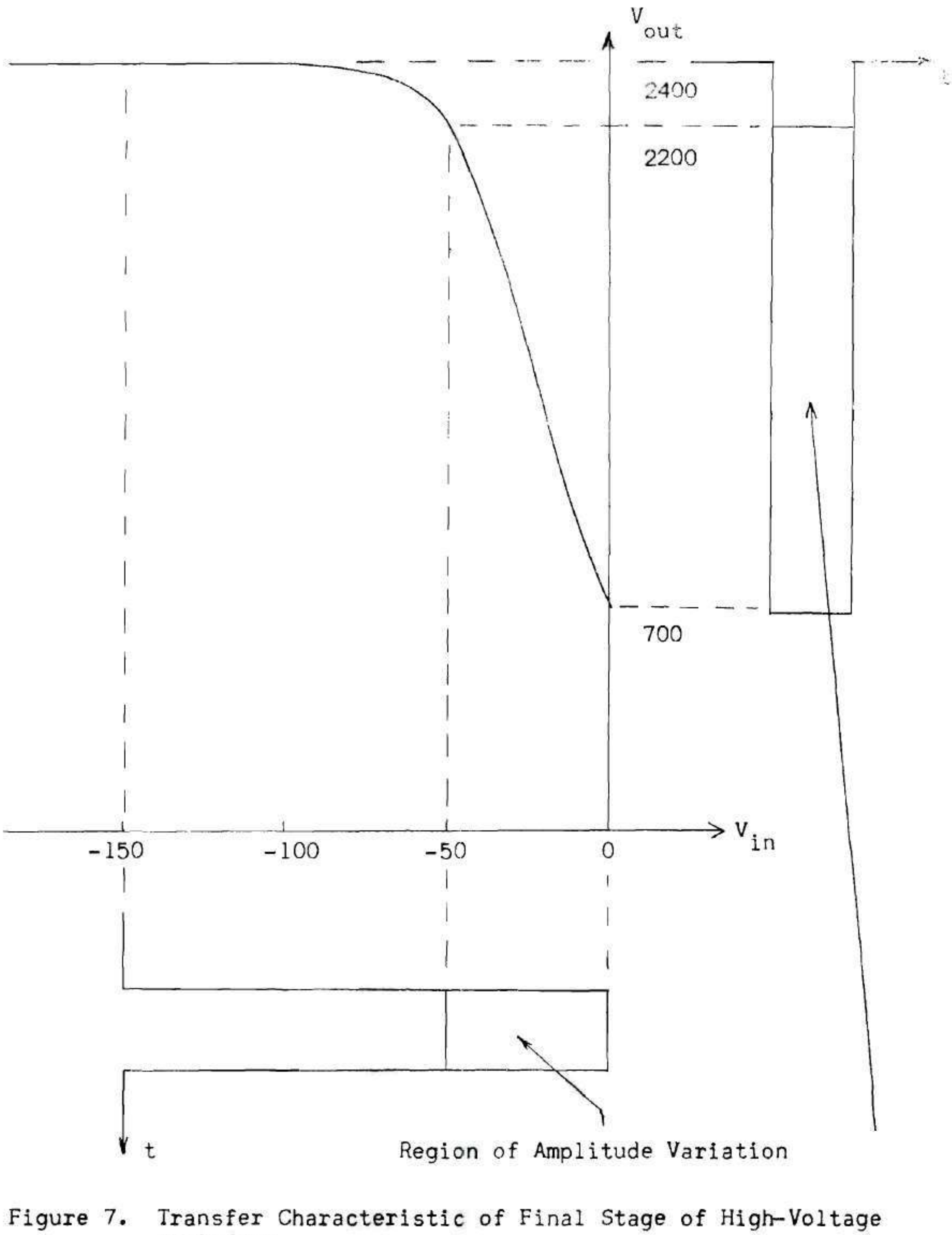

Figure 7. Transfer Characteristic of Final Stage of High-Voltage Amplifier.

capacitor, the KDP crystal, the useful output power was essentially zero. It was unfortunate that the plate load resistance had to be of a low value in order to obtain the necessary wide bandwidth response. Even though the use of cut-off bias reduced the power expended considerably, the current swing capability of the 813 tube placed a lower bound on the plate load resistance of about 5 K-ohms. This was the value chosen. The output capacity of the 813 in parallel with the KDP crystal then produced an RC time constant of approximately 200 nsec. The complete amplifier circuit may be found in the appendix.

The Photodetector

A photomultiplier tube is a device which combines a photo-sensitive cathode with a multi-electrode secondary-emission current amplifier. The current amplification factor is controllable over a very wide range by varying the DC voltage to the divider network supplying the successive current multiplying electrodes. An RCA 7102 photomultiplier tube was chosen as the light detector. This tube has an output current response which is independent of load resistance up to several meg-ohms and independent of the frequency of light modulation to approximately 100 mc. Operated with a 200 K-ohm divider network, as it was, the response is a linear function of incident light intensity over the permissible range of output current, 0 - 10 μamps.

In the construction of the receiver system, the photodetector was allowed to be physically remote from the wide-band amplifier and demultiplexer by use of a 50 ohm coaxial line. In order that the line could be properly terminated without forcing the photomultiplier anode load to be only 50 ohms, a two stage emitter follower circuit was incorporated in the detector chassis to provide a 5.75 K-ohm anode load. The circuit, which is given in the appendix, was designed so that the average anode current level could be monitored by a vacuum tube voltmeter without affecting the AC response and so that 28 mc interference could not be introduced by the DC leads. The low frequency 3 db point due to the output coupling capacitor was 16 cps. Other system components were designed with low frequency break points of from 5 to 10 cps.

It will be recalled that orientation of the quarter-wave plate allowed a choice of two operating points as was shown in Figure 2. By choosing

$$\Delta\psi_o = -\frac{\Pi}{2}, \tag{1}$$

the linear part of the response curve about the operating point was made to have a negative slope. In this way the negative-going output pulses of the high-voltage amplifier produced increasing intensity light pulses. This condition was desired so that the detector current pulses could be allowed to exceed the maximum average current allowable, if necessary. However, this additional gain capability of the photodetector circuit did not prove to be required.

The photomultiplier tube output signal taken across an anode load consisted of negative pulses. When the system was operated at maximum level audio input and the photomultiplier sensitivity was adjusted for an average current of 6 μamps, the maximum output signal variation developed across the 50 ohm load by the emitter follower circuit was 22 mv.

<u>Other Receiver Components</u>

The wide-band amplifier, the demultiplexer, the audio filters, and the audio amplifiers were all incorporated in one chassis and will be described together. The transistor gates, which served to decommutate the received signal and which received their control pulses directly from the multiplexer chassis, were designed for pulses with a maximum amplitude of 2.5 volts. Thus a three stage linear transistor amplifier was built to amplify the 22 mv pulses delivered by the photomultiplier tube chassis to the required 2.5 volt maximum. Linearity and wide bandwidth were enhanced by using emitter degeneration in the common emitter configuration. As was noted earlier, an L-C trap was built into the chassis at the input to this amplifier to eliminate 28 mc interference.

The Fourier spectrum of a PAM waveform, such as the ones obtained from the gates, contains a very strong sample frequency component. The Western Electric filters used in the multiplexer proved to be sufficient to suppress the unwanted lower sideband of the 10 Kc sample frequency but not the sample frequency itself. Sample frequency rejection was improved by employing simple R-C filtering in addition to the Western Electric filter, but as a result the 3 db bandwidth of the audio output was reduced. The addition of a stage of audio amplification in each channel completed the system, giving a root-mean-square output of 0.5 volts for a maximum input sinusoidal signal in the pass band. All circuits are given in the appendix.

CHAPTER III

SYSTEM EVALUATION TESTS

Test Conditions

The conditions under which the evaluation tests were made, except where noted, are given as follows. The sample frequency equaled 10 kc. The duration of both the samples and the off-time between them was 2 μsec. The input signals were sinusoidal with amplitudes approximately equal to 2 volts rms, sufficient to drive the multiplexer output pulses between the minimum and maximum limits of three and five volts. The PM tube sensitivity was adjusted to give 6.0 μamps average anode current, although frequent adjustment was necessary due to laser intensity drift.

Noise and Interference

When a 70 cps sinusoidal signal was applied to the channel B multiplexer input, the receiver rms output voltage of channel B was measured with a narrow-band wave analyser to be 580 mv. Without any input signal present, data were then taken to plot a spectrum of the undesired noise and interference in the output of channel B. On the lower ranges required for most of the data the reading of the meter was made difficult by needle fluctuations of about the same magnitude as the values actually recorded. It was established, however, that these fluctuations were due to the signal being observed rather than due to noise in the wave analyser. The data was later used as recorded in millivolts in the nonlinearity test, but it is presented in Figure 8 in the form of per cent of the nominal 580 mv signal.

Additional tests were made to help interpret the graph shown in Figure 8. First the system was left in operation and the photodetector was blocked. The spectrum then consisted of only a very small amount of flat wide-band noise with one small spike at 60 cps. This test showed that most of the undesired signals did not originate in the receiver after detection. Next the spike frequencies shown in Figure 8 were rechecked twice — once with the system operated as before and again with the modulator removed from the beam and the photomultiplier tube readjusted for 6 μamps average anode current. The results of the second check showed that, within the reading accuracy of the analyser, all of the spikes and bumps in the spectrum were contributed by variations in the laser beam itself and not by the modulation system or the receiver.

The following instruments were used in the preceding tests: a General Radio 736-A Wave Analyser with voltage accuracy given as 5 per cent and response 60 db down at 30 cps off center frequency; a Hewlett Packard 410-A VTVM as the photomultiplier tube monitor; a HP 200-CD Audio Oscillator for the sample frequency; and a HP 200-A Audio Oscillator for the input signals. The frequency range of the HP 200-A was 35-35,000 cps.

Frequency Characteristics

The audio analyser may be read directly in decibels as well as in volts. The input signal supplied by the HP 200-A oscillator was varied in frequency from 35 cps to 10 Kc, and the output was measured with the wave analyser in db below the value measured at 200 cps. Although this

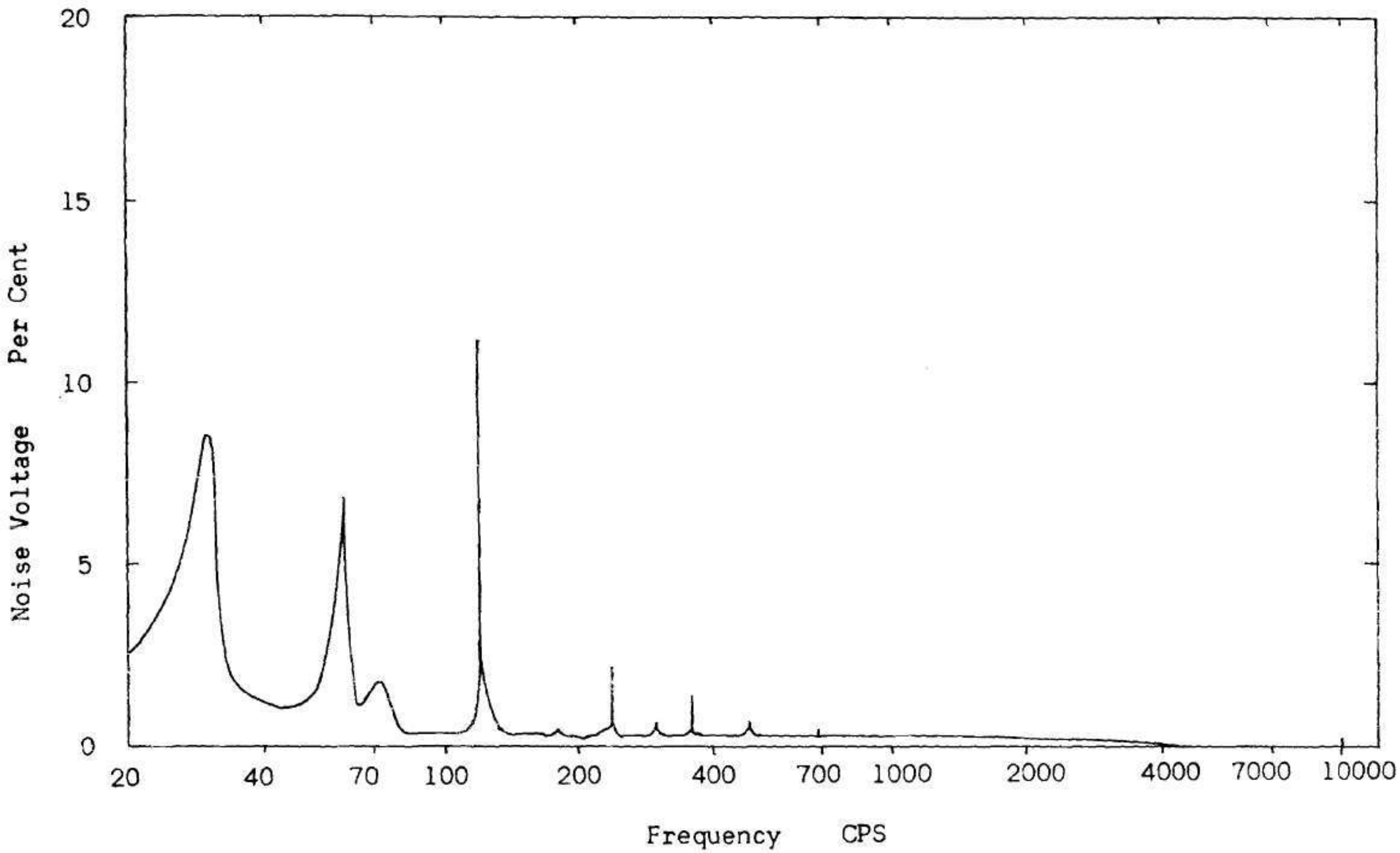

Figure 8. Per Cent Noise Voltage Spectrum of Audio Channel B.

test was performed separately for each audio channel, the results were negligibly different so only the characteristic for channel B will be presented. This graph is given in Figure 9.

The peculiar "shelf" which appears in the graph is the result of a dip in the Western Electric filter characteristic. The roll-off prior to 3 Kc is due to the R-C filters employed in the receiver. Although not shown in the graph, the 10Kc sample frequency was measured to be 50 db down in both channels. It may be noted that the data-point frequencies were chosen to avoid the interference spikes observed in the preceding test.

Nonlinearity

It was desired to characterize the system nonlinearity by finding the coefficients of a truncated power series representing the voltage transfer relation between input and output. To do this it was assumed that the output voltage for frequencies in the pass band was given by a fourth degree equation

$$e_{out} = k_1 e_{in} + k_2(e_{in})^2 + k_3(e_{in})^3 + k_4(e_{in})^4. \qquad (1)$$

The coefficients, k_i, were to be found experimentally.

If one assumes that e_{in} in (1) is given by

$$e_{in} = V (\cos 2\pi f_1 t + \cos 2\pi f_2 t) \qquad (2)$$

and then expands (1) trigonometrically, one would find that the output under such signal conditions would contain sum and difference frequencies of f_1 f_2. The coefficients of the various frequencies present would be algebraic

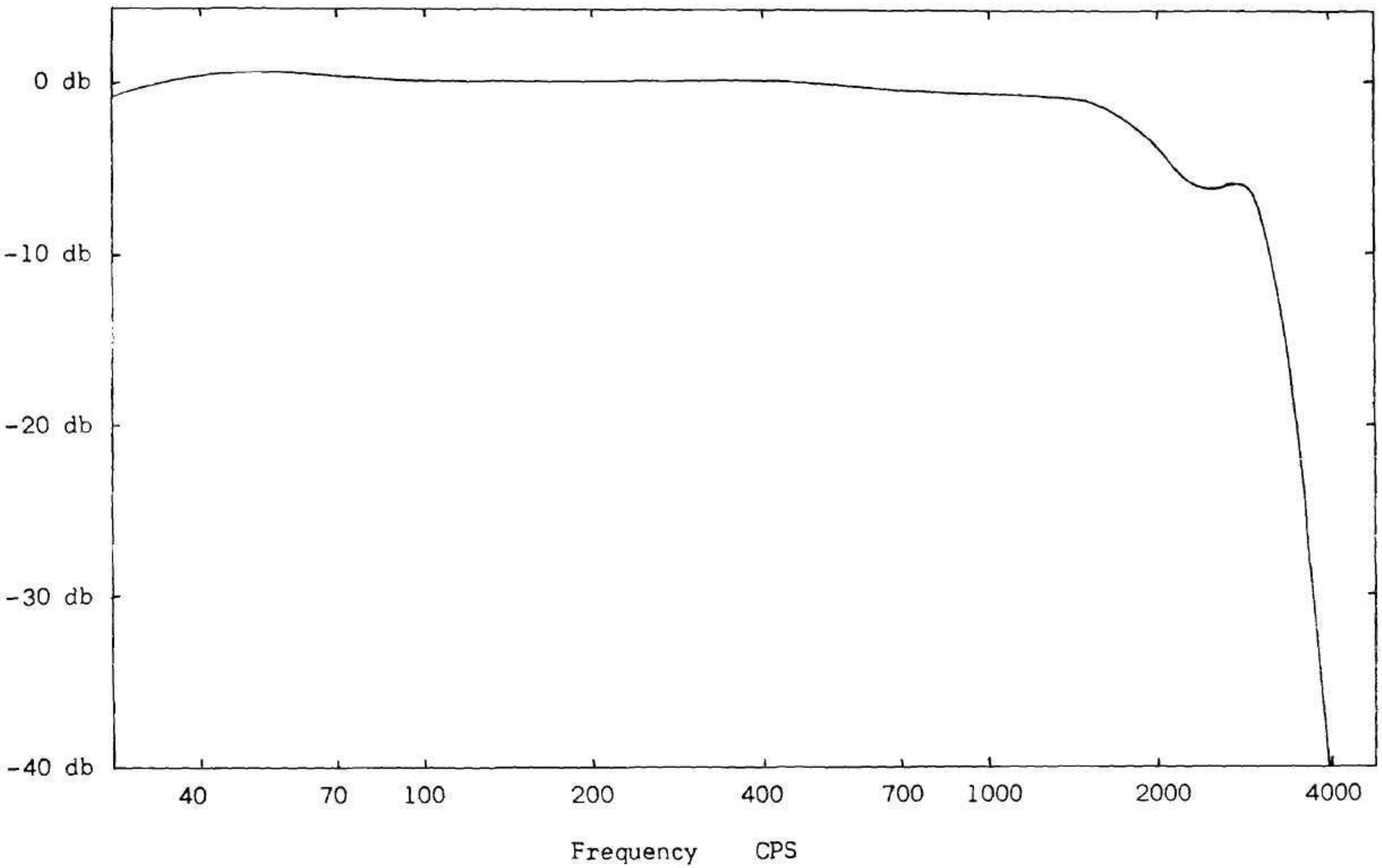

Figure 9. System Frequency Characteristic.

combinations of the coefficients in (1). By operating the system with an input signal as given by (2) and measuring the coefficients of the trigonometric expansion of (1), the coefficients k_i could be calculated.

Two frequencies were chosen, 500 and 700 cps, so that none of the sum and difference frequencies of interest would lie within 30 cps of each other or within 30 cps of noise and interference spike frequencies. This choice was made so that the wave analyser would give 60 db rejection of undesired signals. The amplitude, V, of each input component of channel B was adjusted to 1.56 volts, the value which caused the sum signal to have the maximum allowable peak-to-peak swing. A careful search for the expected sum and difference frequencies revealed that most of them were lost in the small wide-band noise present, and that the maximum signal found was approximately 39 db below either of the desired components, f_1 and f_2.

As was the case in measuring the noise spectrum, the meter needle fluctuations made data taking difficult. In a typical instance the meter needle fluctuated mostly between 3 and 7 mv. The noise at a frequency 30 cps removed from this signal caused fluctuations between 1/2 and 4 mv. The values recorded in these instances were 5 mv and 2 mv respectively. Despite the obvious question of accuracy, the recorded values were used to determine a third order expression for the system transfer characteristic.

$$e_{out} = 0.27\ e_{in} + 0.002\ (e_{in})^2 + 0.001\ (e_{in})^3 \qquad (3)$$

Thus nonlinearity was not a serious defect of this system.

Signal Waveform Study

System Waveforms

A Tektronix 545B oscilloscope with the 1A1 dual-trace plug-in unit was employed as a means of observation and measurement of the waveforms present at various points in the system. The oscilloscope rise time with P6006 10x probes was given by the manufacturer as 11 nsec, and voltage calibration was given as 3 per cent. Input impedance with the probes was 10 meg-ohms paralleled by 7 $\mu\mu$fds, and the maximum allowable input voltage was 600v.

Permanent records were made of the waveforms with a Dumont 302 Oscillograph Record Camera. The film was Polaroid, type 47, and the shutter conditions were f 2.8 and 1/25 sec. Some of the pictures are presented in Figure 10. It should be noted that the oscilloscope camera inverted the horizontal scale in these photographs so that increasing time is to the left.

Picture (a) in Figure 10 compares the multiplexed signal prior to amplification, shown in the bottom trace, with the inverted output of the high-voltage amplifier. Because of the time scale inversion, channel A is to the right, followed by channel B to the left. The sweep rate was 1 μsec/division; sensitivity was 5 volts/division on the lower trace and 200 volts/division on the upper trace. Due to the 600 volt maximum input limitation of the oscilloscope a voltage divider was used to reduce the high-voltage output signal to the 400 volt maximum shown in the picture. Calculations which took into consideration the loading effect of this voltage divider showed that the reduction ratio was 4.2:1 and that rise times should have been less than 3 per cent in error.

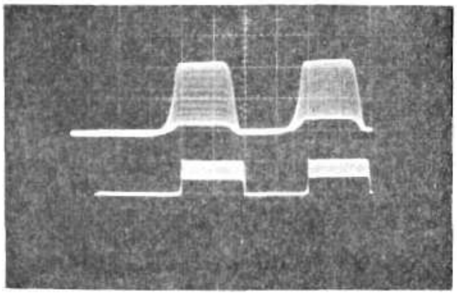

(a)

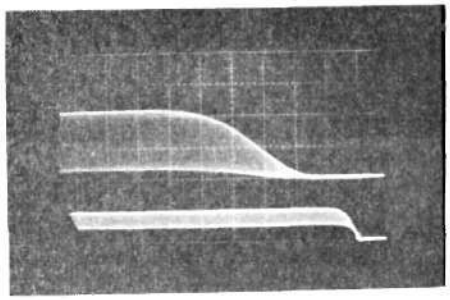

(b)

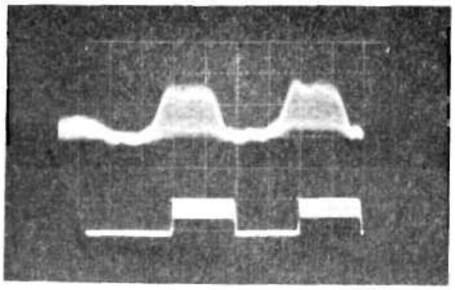

(c)

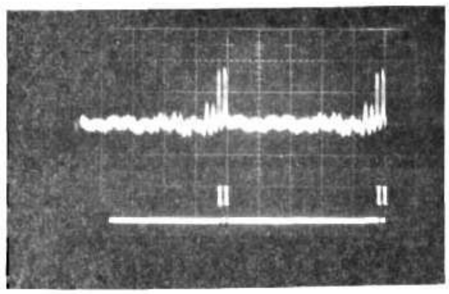

(d)

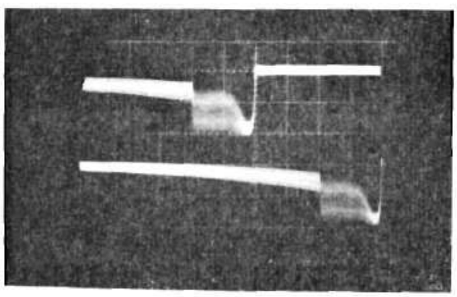

(e)

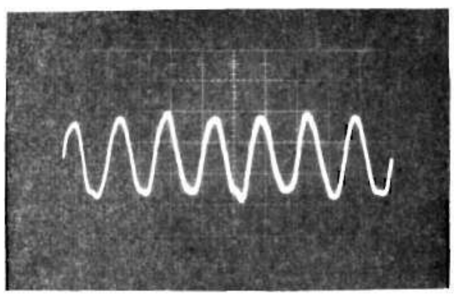

(f)

Figure 10. Oscilloscope Photographs of System Waveforms.

Picture (b) was taken under the same conditions as (a) but with a sweep rate of 0.1 μsec/division. In these two pictures one can note first the pedestal previously mentioned in the lower trace and its near absence, after class C amplification, in the upper trace. Taking into account the reduction factor, one may calculate the gain of pulse amplitude variation in the high-voltage amplifier to have been 630. It may also be seen that while the rise time of the transistor multiplexed pulses was only 25 nsec the rise time after amplification was 300 nsec. If one measures pulse delay from the half-rise point, the amplifier delay was also about 300 nsec.

Photograph (c) shows the high-voltage pulses replaced with the received light signal after it had been detected and amplified for gating. The lower trace was again taken from the multiplexer output for comparison. The upper trace was made with a sensitivity of 2 volts/division. The effects of wide-band receiver noise are noticeable in the upper trace, and it may be seen that the delay had increased to about 500 nsec.

Picture (d) was taken under the same conditions as those for (c) but with sweep rate slowed down to 20 μsec/division. In this picture almost two entire sample frames are visible. The bottom trace is still the multiplexer output, and it shows that the spacing would allow 23 more channels per frame. Of great importance is the fact that the received frames recorded in the upper trace show that two additional pulses were received which did not correspond to any electrical modulating signal. Further it may be seen that some transient ripple was present throughout the entire frame. A more careful study of these effects will be presented in the next section.

Photograph (e) in Figure 10 was taken under the same conditions as (c) but with the two oscilloscope probes on the output of the demultiplexing gates. The lower trace shows channel A gated, and the upper trace shows channel B gated. Since the gating pulses were negligibly delayed, these traces show the total delay of the signal pulses. The exponential rise to the left of each received pulse was a result of initial R-C filtering.

The last picture, (f), was taken with sweep rate of 1 msec/division and sensitivity of 1 volt/division. The probe was on the audio output of channel A. The effects of noise and interference are visible as waveform distortion of the original 670 cps sine wave input signal.

Crystal Effects

As has been stated, KDP crystals are piezo-electric in nature and may be mechanically stressed by electric signal voltages on the field electrodes. Unfortunately, the mechanical stresses so produced can cause modulation in a KDP modulator. The strange appearance of the received frames shown in Figure 10 (d) was attributed to such mechanical effects, and further pictures were made to study them more closely.

In Figure 11 photograph (a) shows one received frame before amplification, recorded with a sweep rate of 10 μsec/division and a sensitivity of 10 mv/division. For clarity the picture was made with only one channel pulse train activated and that with no amplitude modulation. Picture (b) was taken under the same conditions as (a) but with both pulse trains activated. These pictures show clearly that undesired delayed pulses were received. The known facts strongly suggest that these secondary pulses were due to mechanical crystal transients. Had a third channel

(a)

(b)

(c)

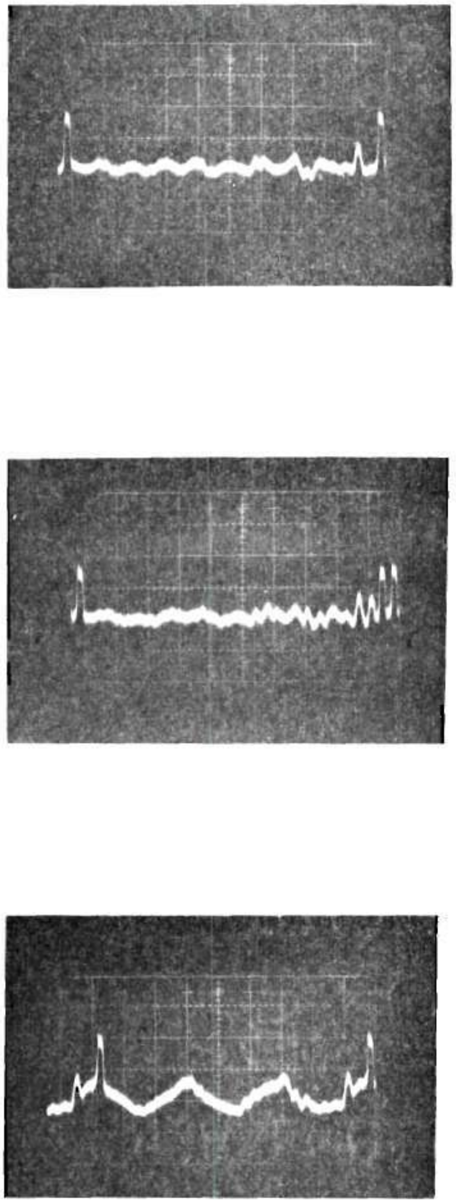

Figure 11. Oscilloscope Photographs Showing Crystal Effects.

been implemented in this system, its pulses would have fallen exactly on top of the transient pulses from the first channel. That this would cause a cross talk problem will be seen in the next section.

The JX-1 manual had indicated that the fundamental piezo-electric resonance of the crystal should have been approximately 48 Kc. Pulse waveforms such as those of a TDM system contain strong harmonics of the sample frequency, and these were used to find the fundamental resonance. By varying the sample frequency with only one unmodulated channel activated, the resonance was found to occur at the third harmonic of 11.8 Kc and at the fourth harmonic of 8.8 Kc, that is, at 35 Kc. Picture (c) in Figure 11 was taken with the sample frequency at 11.6 Kc because it was feared that a sustained signal at 11.8 Kc might damage the crystal. In this picture three periods of the fundamental vibration may be counted. It will be seen that cross talk might occur for sample frequencies so chosen.

Cross Talk Investigation

Cross talk refers to the reception in one channel of the signals transmitted in other channels. In a TDM-PAM system it usually results from incomplete decay or nullification of the transients from the pulses preceding the one of the channel in question. In the constructed system, the channel B pulses followed immediately the channel A pulses so cross talk was much larger in channel B than in channel A. It was therefore decided to measure only the cross talk in channel B.

To obtain a measure of the cross talk, the following procedure was used. The input signals of channels A and B were supplied by two HP 200-A oscillators at 400 cps and 300 cps, respectively. These frequencies were chosen in the flat part of the audio pass band away from the large interference spikes. The input amplitudes were adjusted so that the desired output signal amplitudes in the two channels were equal, as measured with the wave analyser. This adjustment required that the input amplitudes be slightly unequal due to small differences of gain in the output audio amplifiers. The wave analyser was then used to measure the amplitude of the undesired 400 cps signal in the channel B output as a per cent of the desired 300 cps signal amplitude.

Cross Talk Vs. Sampling Frequency

Ordinarily one would not expect the pulse transients to be dependent on the sample frequency in a TDM system. As was previously noted, however, crystal effects caused the transmitted waveform to be very dependent on the sample frequency. Thus cross talk data was taken with the sample frequency as a parameter from just above the 8.8 Kc resonance to just below the 11.8 Kc resonance. The test was made with the off time between pulses at the nominal 2 μsec and then repeated for off times of 1.5 μsec and 2.4 μsec. However, the resulting data was negligibly different in the latter two instances from that in the first so only the data from the 2 μsec case is presented in Figure 12. It may be observed in this graph that there was a cross talk null for a sample rate of 10.2 Kc.

Cross Talk Vs. Pulse Spacing

Cross talk data was also taken with the off time between pulses, t, as a parameter, and the resulting graph is shown in Figure 13. In this test the sample frequency was set at 10.2 Kc, the null found previously. This same null may be seen in Figure 13 at the point, $t = 2$ μsec.

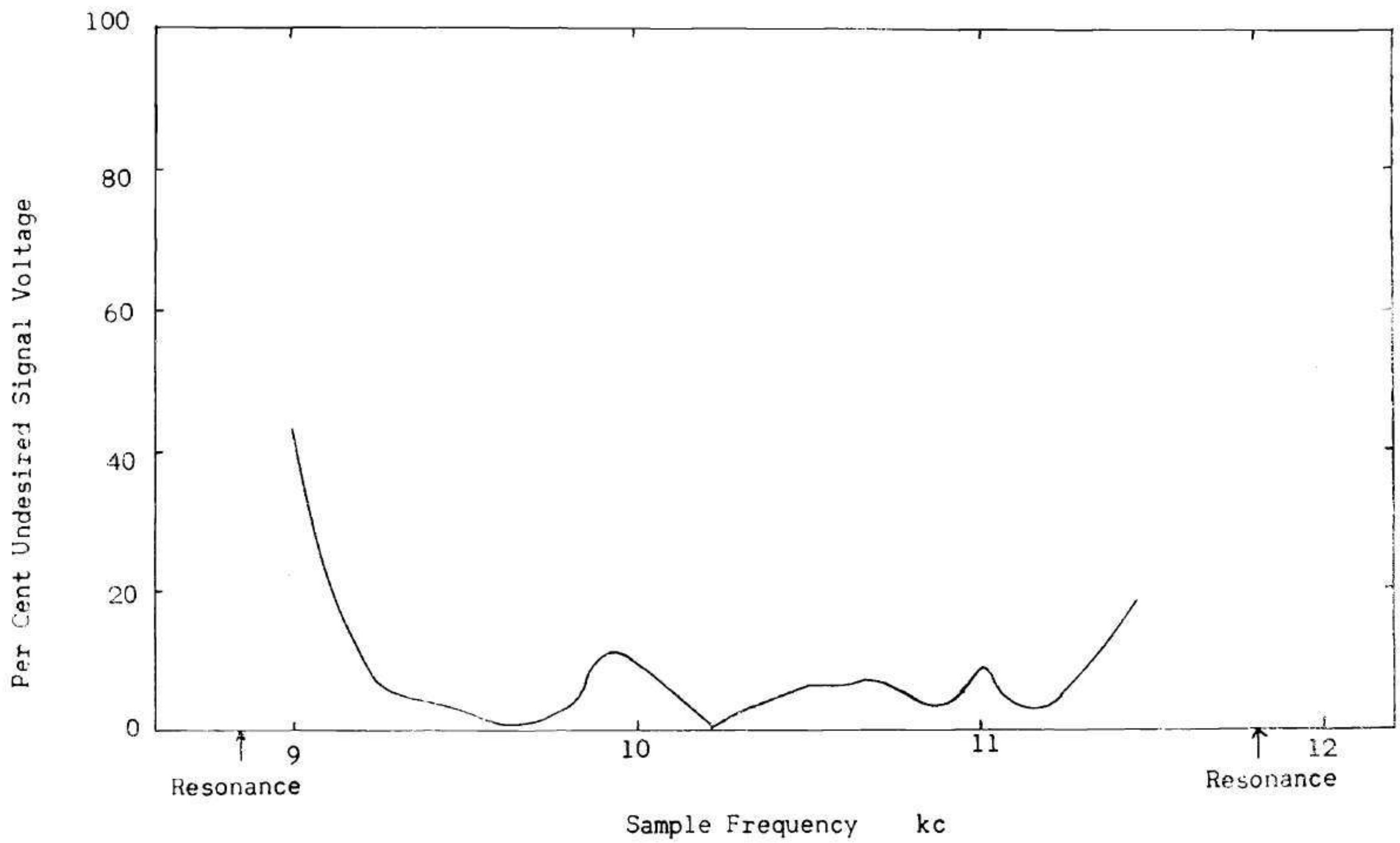

Figure 12. Per Cent Cross Talk Measured in Channel B Vs. Sample Frequency.

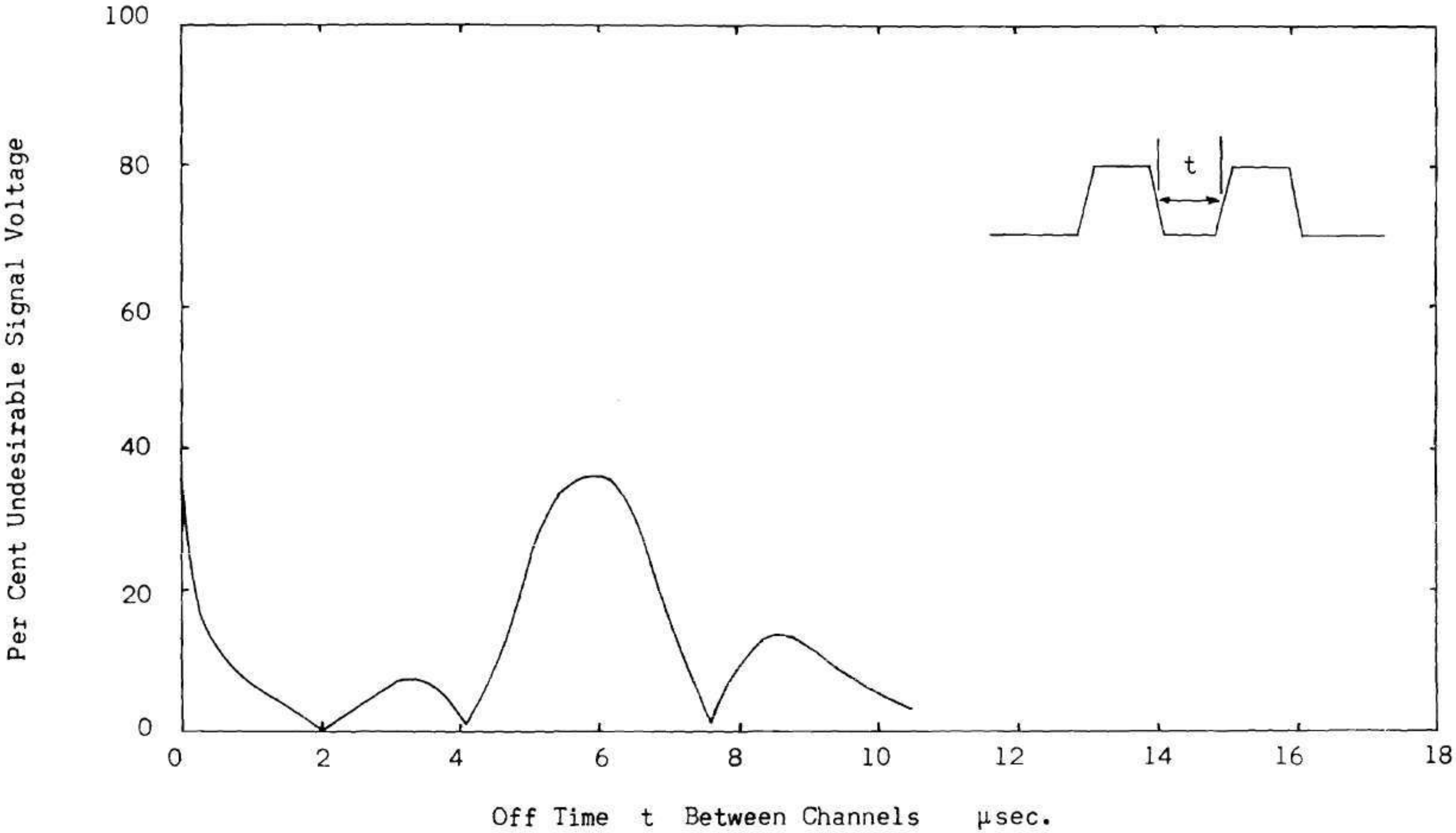

Figure 13. Per Cent Cross Talk Measured in Channel B Vs. Off Time Between Pulses.

As was expected, the cross talk became more severe as the time t approached zero. The dramatic result, however, was that a large cross talk maximum occurred for $t = 6\ \mu sec$. The waveform photographs in Figure 10 of the last section show that this cross talk maximum corresponded exactly to the undesired secondary pulse believed to be produced by the crystal transients.

The Voice Test

The system was subjectively tested by simultaneous transmission of two male voice readings. First the voices were recorded on the separate tracks of a stereo tape with an Ampex 351-2 stereo recorder-reproducer. This machine then provided the inputs for the system. The output levels of the reproducer channels were adjusted so that the audio voltage peaks exceeded the nominal limits of the system. Unfortunately the only other available tape recorder was an Ampex 600 portable which was not capable of two track recording. Both output channels were recorded, however, by recording one and then replaying the stereo input tape and recording the other.

The output tapes were compared with the input tapes by playing them sequentially through an Ampex 620 Amplifier-Speaker. The subjective opinion of several people was that the output was quite intelligible and recognition was good. The absence of high-frequency response was notable as had been expected. Both noise and interference hum were present to limited extent, but cross talk could not be detected by ear. The 10 Kc sample frequency was barely detectable, if one listened for it.

CHAPTER IV

BASIC SYSTEM LIMITATIONS

In this chapter two types of system limitations will be discussed. The first section will deal with effects which were observable in the constructed system. In the second section some limitations will be pointed out that would affect systems of greater bandwidth.

Discussion of Results

Laser Effects

In Chapter III it was shown that the intensity of the laser beam was already modulated with undesirable audio signals before modulation by the experimental system. Although the laser was only crudely shock mounted, the fact remains that lasers are extremely sensitive to vibration. The relative magnitude of the laser-introduced background noise in the experimental system would be acceptable in a military voice communications link, perhaps, but the high quality transmission of music would require very much better laser mounting. This problem would become even more severe if, for other reasons, a lower per cent modulation were deemed necessary.

Detector Noise

In the laboratory system the total distance of transmission was only five feet; still, there was a quite audible amount of wide-band noise in the received audio output which was generated by the receiver itself. This noise was mostly the result of very-wide-band shot noise from the photomultiplier tube.

There are several ways in which the output signal-to-noise ratio might be improved. One certain way would be to first shape the transmitted pulses for minimum bandwidth requirements and then incorporate a wide-band, low-pass filter in the receiver prior to demultiplexing. Downing[11] treats such "base-band filtering" and other schemes for improving signal-to-noise ratio in TDM-PAM systems. The photomultiplier tube is a noisy detector, but it has high sensitivity and great bandwidth. It is possible, however, that other forms of light detection can provide better signal-to-noise characteristics. An obvious final suggestion for an investigator of optical TDM systems is that other forms of pulse modulation, such as PDM, PPM, or PCM, could give better output signal-to-noise ratio than PAM, although at the expense of some bandwidth.[11]

Modulation Power

Although not discussed as an evaluation result, the question of the high-voltage amplifier output power arose in the design of the system. It is presented here with a simple model to demonstrate a general relation between power, achievable pulse rate, capacitance, and voltage parameters of the crystal. In this discussion the KDP crystal modulator will be considered electrically as an ideal lossless capacitor. It will further be assumed that in a wide-band pulse system the energy expended in charging the crystal capacitance to the desired voltage may not be conserved.

The model to be used is the following one. An ideal controlled current source is loaded by a resistance, R, in parallel with the output shunt capacity, C, which includes the crystal capacity. The output current consists of a uniform rectangular pulse train of amplitude I_{max}

whose pulse duration is 5 RC and whose spacing is also 5 RC. Thus the output voltage pulses are nearly rectangular and reach a maximum given by

$$V_{max} = I_{max} R \ . \tag{1}$$

The amplification is considered to be such that V_{max} is the rms value of peak pulse voltages which would be used in a real TDM system. Moreover, V_{max} would be chosen as some $k\ V_{\Pi}$, where V_{Π} was the half-wave retardation voltage and k was some constant fraction less than one.

From the assumed pulse shape the pulse rate, W, follows immediately as

$$W = \frac{1}{(2)\ (5RC)} = \frac{1}{10RC} \ . \tag{2}$$

The output power of the amplifier may be approximated by assuming the voltage waveform to be exactly rectangular and calculating the energy delivered per pulse from

$$U = \frac{(kV_{\Pi})^2}{R}\ (5RC) + \frac{C}{2}\ (kV_{\Pi})^2 \ . \tag{3}$$

The power delivered by the current source is then

$$P = WU = W\ [5Ck^2V_{\Pi}^2 + \frac{C}{2}\ k^2V_{\Pi}^2] \ . \tag{4}$$

Now, it is true that other waveshapes and more sophisticated circuit design could reduce the required power, and perhaps a better practical estimation would be only half of that given in (4). At any rate, for a nonconservative system, a theoretical lower bound can be given as

$$P_{min} = Ck^2 V_{\Pi}{}^2 W \quad . \tag{5}$$

It should be pointed out here that work is currently being done on transverse Pockel's effect modulators. In such modulators the modulating field is applied perpendicular to the beam, and V_{Π} is inversely proportional to the length of the crystal. The capacitance is proportional to the length. Equation (5) shows that, for such a modulator, power reduction would result from increasing the modulator length.

The essential point to be made is that both the per cent modulation and the crystal half-wave voltage enter the power expression squared. Because of this fact, the design of a very high rate pulse modulator should sacrifice increased capacitance for lower V_{Π} if possible. Furthermore, when considering signal-to-noise ratio and per cent modulation it should be remembered that lowering k will result in transmitter power savings proportional to $(k)^2$.

Crystal Transient Effects

It was observed in Chapter III that unacceptable amplitude modulation occurred due to piezo-electrically induced mechanical stresses in the crystal. This piezo-optic effect, as it is called, is exhibited by all Pockel's-effect crystals of the KDP type, that is, of symmetry class $\bar{4}2m$. Stephany[12] shows that these crystals may exhibit strong resonances up to approximately the 1000th harmonic of the fundamental resonance frequency if rigid mounting is not used. However, the JX-1 manual[9] states that "... the laminated cover glasses and mount severely damp the resonant vibration." The results, then, indicate that even with firm mounting the piezo-optic effect will produce a very serious problem for a high-rate TDM-PAM system design.

Before abandoning the idea of pulse amplitude modulation altogether, a designer should investigate several possibilities. The piezo-optic effect is relatively more pronounced in some materials than in others. Ammonium dihydrogen phosphate, or ADP, exhibits the effect to a greater degree than does KDP, but more recently discovered modulating materials may not. A thorough study of crystal shapes and mounting methods to minimize the effect should be made. It could well turn out, however, that it is not feasible to reduce the crystal-introduced cross talk to an acceptable level for a TDM-PAM system. Should this be true, it would appear that one of the other pulse modulation systems, which are relatively insensitive to amplitude variations, would solve the problem if the extra bandwidth necessary were available.

Discussion of Other Effects

Modulation Mathematics

In Chapter I it was stated that the detector current in a system employing a KDP modulator with a quarter-wave retardation plate and a square-law detector could be given as

$$I = \sin^2\left(\frac{\Pi}{2}\frac{V_m}{V_\Pi} \pm \frac{\Pi}{4}\right) \tag{6}$$

where V_m was the modulating voltage. Expression (6) may also be interpreted as the intensity, I, of the modulated light beam. This mathematical model was quite sufficient for the constructed system, but it would break down at higher frequencies and thus needs some refinement. In the derivation of (6) it is assumed that the modulating electric field within the crystal does not change appreciably during the transit time of a photon passing through the crystal. This assumption would not be valid if the pulse waveform bandwidth extended to the gigacycle range.

Holshouser, Von Foerster, and Clark have written a paper called "Microwave Modulation of Light Using the Kerr Effect."[13] The mathematics of the Kerr effect modulator are similar to those of the Pockel's effect modulator. The difference lies in the fact that, in the Kerr effect, phase retardation is proportional to the square of the modulating field instead of being a linear effect. It should not be too difficult a task to modify the integrals and transformations given in the paper mentioned to predict the response of a Pockel's modulator to gigacycle rate pulse trains. However, this task will not be undertaken here.

Multiple Carrier Frequencies

There is another effect, not accounted for by (6), which occurs at modulating frequencies an order of magnitude smaller than those involved in the transit-time effect mentioned above. In the derivation of (6) it is assumed the light beam is truly monochromatic, that is, its electric field strength may be represented by a single-frequency sinusoidal vector function of time which is independent of position on a plane perpendicular to the direction of the beam. As a result of this assumption, the field strength of the linearly polarized output beam may be represented at one point in space and in one direction by

$$E(t) = E_o \cos w_o t \sin \left(\frac{\Pi}{2} \frac{V_m}{V_\Pi} + \frac{\Pi}{4} \right) \qquad (7)$$

where $\frac{w_o}{2\Pi}$ is the single light frequency. Squaring (7) and neglecting the constant multiplier and the $2w_o t$ term gives (6).

Unfortunately, most laser beams do not obey the above assumption, because they contain several distinct frequencies instead of just one. The 6328 Å helium-neon laser is an oscillator which uses a multimode cavity resonator and an amplifying medium whose bell-shaped frequency characteristic encompasses several modes. If the laser is operated with only longitudinal modes present,[14] the output beam will contain discrete frequencies spaced nearly uniformly in the pass band by an amount

$$\Delta f \approx \frac{c}{2d} \quad . \tag{8}$$

Here c is the speed of light and d is the spacing between the laser mirrors. The total width of the pass band, while negligibly small in terms of the light frequency, is still approximately 1000 mc. This is sufficient for about 10 different light frequencies to exist in the output of a 150 cm laser.

Let it be supposed that a modulating signal is given by

$$V_m(t) = V_s \cos w_s t \tag{9}$$

where

$$\frac{1}{2\pi} w_s < \Delta f \tag{10}$$

and that the laser beam field strength is given as

$$E(t) = A_o \cos w_o t + A_1 \cos (w_o + \Delta w)\, t + \ldots \tag{11}$$

$$\ldots + A_n \cos (w_o + n\Delta w)t,$$

where

$$\Delta w = 2\Pi \, \Delta f = 2\Pi \frac{c}{2d} . \tag{12}$$

Then, the modulated output field strength is expressed by

$$E_{out}(t) = \left[\sin \left(\frac{\Pi}{2} \frac{V_s}{V_\Pi} \cos w_s t + \frac{\Pi}{4} \right) \right] \tag{13}$$

$$\cdot \left[\sum_{j=o}^{n} A_j \cos (w_o + j \, \Delta w) t \right] .$$

The light detector is assumed to be a square-law device with a pass band from zero to $2 \, \Delta f$. If one omits the constant multiplier and the frequency terms outside the pass band of the detector, the detected current may be expressed as

$$i(t) = \left[1 + \sin \left(\Pi \frac{V_s}{V_\Pi} \cos w_s t \right) \right] \tag{14}$$

$$\cdot \left[\sum_{j=o}^{n} A_j^2 + 2 \left(\sum_{j=1}^{n} A_j A_{j-1} \right) \cos \Delta wt \right] .$$

For linear response, V_s will have been chosen small enough for the following approximation to hold.

$$\sin \left[\Pi \frac{V_s}{V_\Pi} \cos w_s t \right] \approx \Pi \frac{V_s}{V_\Pi} \cos w_s t \tag{15}$$

After substituting the approximation, (14) may be expanded. The DC terms, constant multipliers, and all frequency terms greater than Δf are eliminated to give the detector current terms of interest.

$$i(t) = \cos w_s t + B_o \cos (\Delta w - w_s)t + \tag{16}$$

$$+ \frac{2V_\Pi}{\Pi V_m} B_o \cos \Delta wt$$

The relative coefficient, B_o, is given by

$$B_o = \frac{\sum_{j=o}^{n} A_j^2}{\sum_{j=1}^{n} A_j A_{j-1}} \quad . \tag{17}$$

The second and third terms in (16) are undesirable. They show that if the modulating signal were a wide-band one, with a highest frequency component greater than $1/2\ \Delta f$, the lower side band of Δf would interfere with the desired signal in the detector output. Thus the useful bandwidth of a system employing a multimode laser may be increased by making the laser shorter and hence increasing Δf.

Another point of interest concerns the factor, B_o, in equation (16). As Δf increases, fewer frequencies remain in the laser pass band and the amplitudes of adjacent frequencies vary more. This causes B_o to decrease to zero as Δf approaches the width of the pass band. In other words, a single mode laser with only one output frequency may be obtained by making the laser short enough, and such a laser would impose no $1/2\ \Delta f$ frequency limit on the communications system. Fortunately, super-mode lasers have recently been reported which produce only one output frequency without suffering the loss of gain which accompanies the use of very short lasers.[15]

Modulator Limitations

In all discussions of power and frequency response the modulator has been assumed to be an ideal lossless capacitor. Such a model would not be valid at all frequencies. A more detailed model shows series inductance and resistance for the leads and electrodes. Even though KDP is a low-loss dielectric, a shunt loss resistor would be necessary for the model at higher frequencies, and at some point lumped circuit models would become totally inadequate.

Electrode or dielectric heating can easily destroy a KDP crystal by thermal stress. In the case of the JX-1 modulator, for example, the frequency limit of a 1500 volt peak sinusoidal signal is 20 mc in a 70° F ambient temperature environment. This limit is imposed by electrode dissipation even though the electrodes are made of solid copper plates.

CHAPTER V

SUMMARY AND CONCLUSIONS

The 10^{14} cps frequency of the optical laser seems to offer the possibility of communications systems with very large information capacity as compared with the systems in use today. For example, if a 1 per cent modulation bandwidth could be achieved, the usable bandwidth would be 10^{12} cps which is enough to frequency multiplex approximately 200,000,000 single-sideband telephone channels. To make use of such a bandwidth with a base-band TDM system would require circuitry with pulse rise times on the order of 10^{-12} seconds. Such circuitry is probably not forthcoming in the immediate future.

There have been many papers on the subject of microwave modulation of light, and it is true that such methods will probably result in more usable bandwidth than will base-band TDM. However, microwave modulation techniques leave a large gap in the modulation spectrum from zero up to the giga-cycle range. It is precisely this gap which may be at least partially filled by base-band TDM systems.

The evaluation of the constructed TDM-PAM system has shown that such systems are feasible. Perhaps the main conclusions drawn from the evaluation have been formulations of some of the important problems which would appear in the design of a practical wide-band pulse system. These conclusions will be stated in the following paragraphs.

Undesired Amplitude Variations

The output amplitude of a laser beam is very sensitive to vibration of the laser mirrors. Any such amplitude variation at audible rates is reproduced in every channel of a TDM-PAM system. If a photomultiplier tube is used as a detector, shot noise from this device will constitute one receiver problem. The JX-1 KDP modulator would be unacceptable for a TDM-PAM system because of the cross talk introduced by piezo-optic transients. A study should be made of crystal shapes and mounting methods to minimize the piezo-optic effect. If the designer could spare the extra required bandwidth, all of these undesired amplitude effects could be considerably reduced by using another form of pulse modulation such as PDM, PPM, or PCM.

Power

An expression for the minimum possible power output of the modulating amplifier in a nonconservative system was given.

$$P_{min} = C\, k^2\, V_{\Pi}^2\, W \qquad (1)$$

In this expression, C is the crystal capacity, W is the pulse rate, and (kV_{Π}) represents the rms value of the output pulse voltage peaks. The fact that voltage appears squared emphasizes the need for low voltage modulators.

In comparison with (1) the losses in the crystal electrodes and dielectric are small. These losses must not be neglected, however, for a KDP modulator may be easily destroyed by the thermal stress due to such dissipation.

Multimode Lasers

The approximate spacing between the output frequencies of a gas laser operated with only longitudinal modes present is given by

$$\Delta f = \frac{c}{2d} \quad . \tag{2}$$

It was shown in Chapter IV that if such a multimode laser is used in any wide-band system, similar to the one constructed, the usable bandwidth will be limited to one half the difference between laser frequencies as given in (2).

APPENDIX

A schematic diagram of the transmitter, which includes audio filtering, sample pulse generation, audio sampling, channel summing, high voltage amplification and light modulation, is given in Figure A1 on the following page.

The receiver, which includes an RCA 7102 photomultiplier tube and associated circuits in a separate chassis connected by 50 ohm coaxial cable to the wide band amplifier, demultiplex gates, audio filters, and audio amplifiers, is shown schematically in Figure A2. Note that the high voltage resistance divider network required by the photomultiplier tube dynodes is not shown. The divider network used was one recommended by the manufacturer. It was constructed with precision resistors totaling 220 K ohms in series.

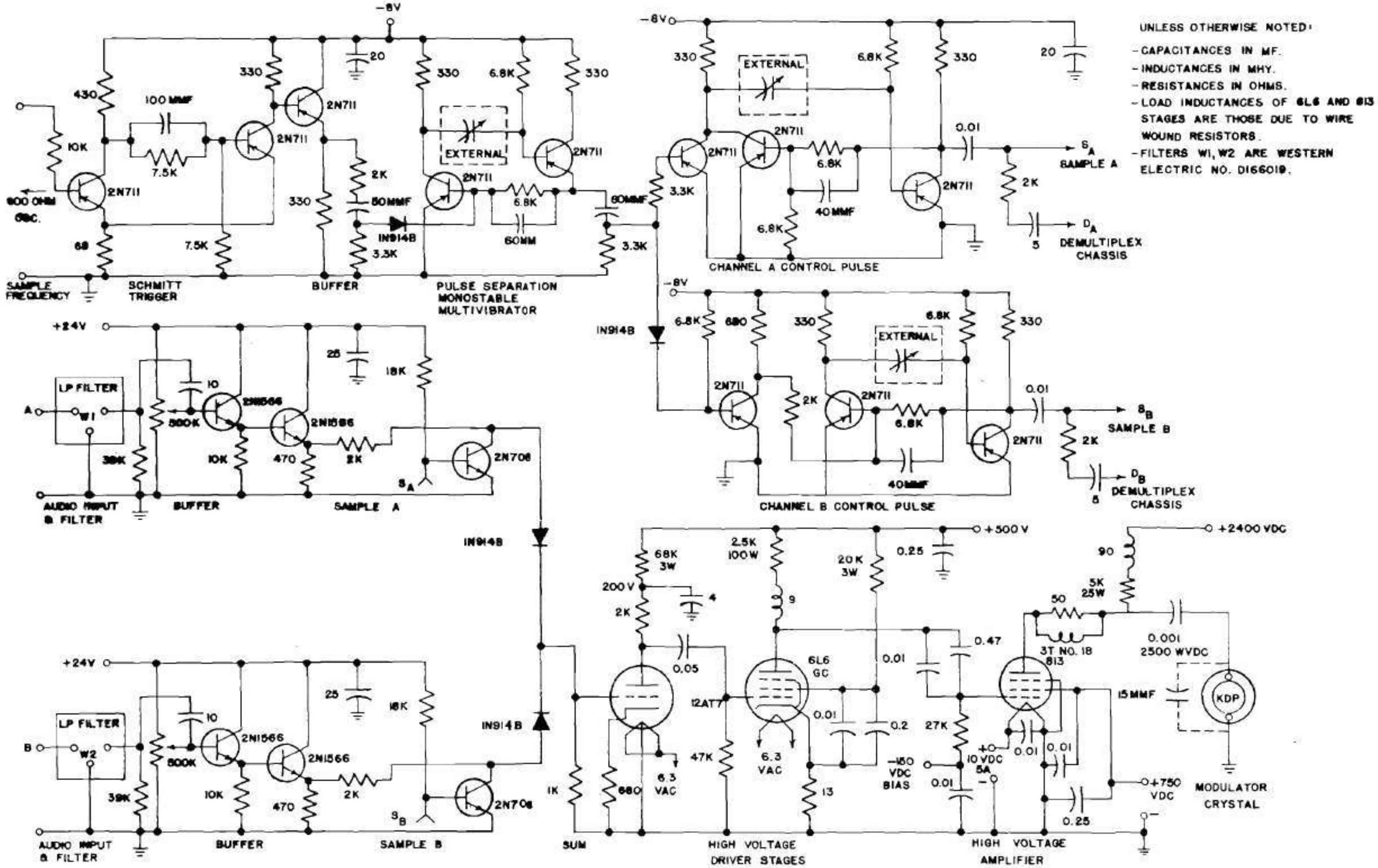

Figure A1. Transmitter Schematic.

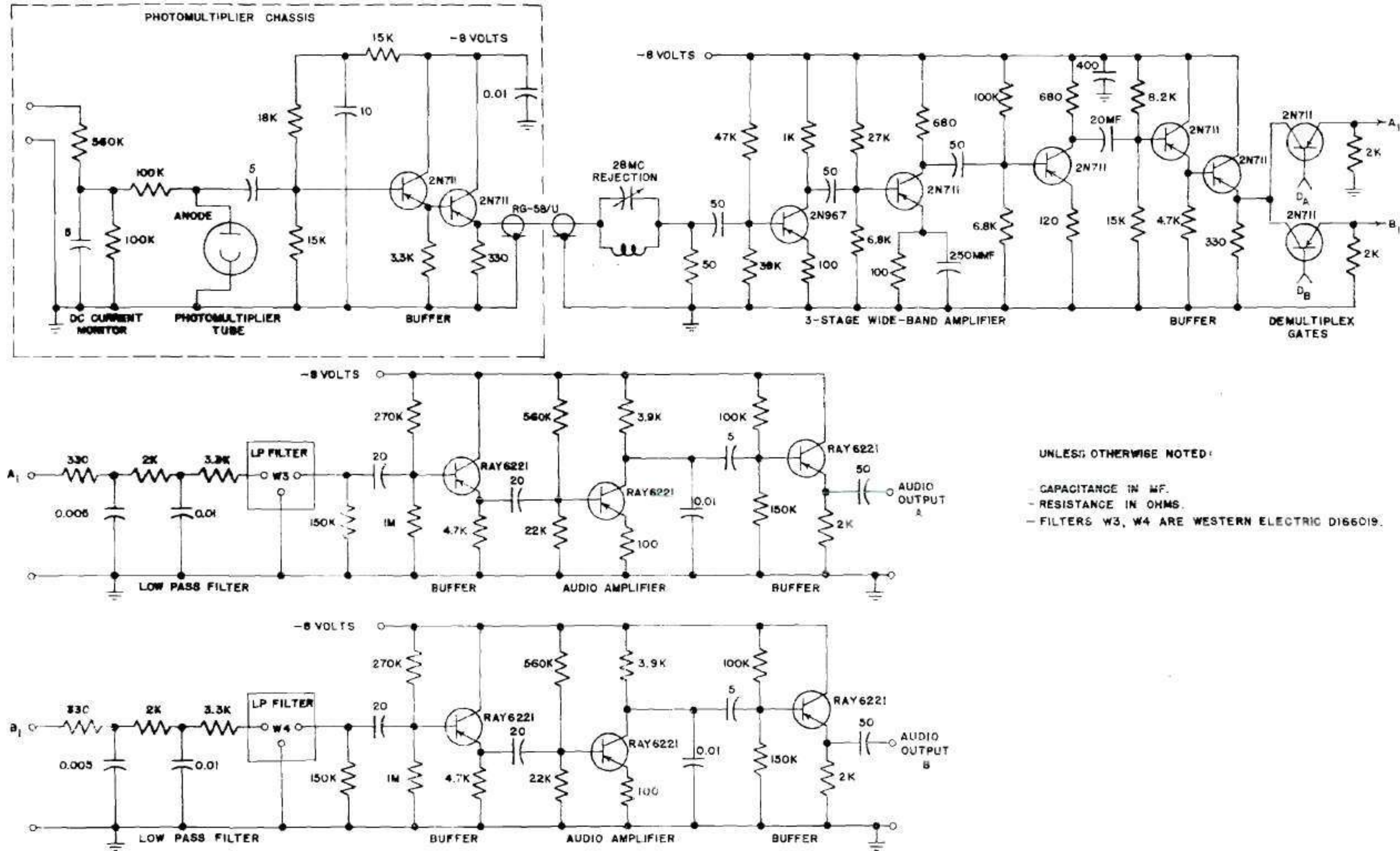

Figure A2. Receiver Schematic.

REFERENCES CITED

1. Kalus W. Otten, "Principles of Optical Communication," Electro-Technology, pp. 112-130, September, 1962.

2. James A. Fusca, "Laser Communications," Space/Aeronautics, pp. 58-77, May, 1964.

3. Mauro DiDomenico, Jr., "High Frequency Modulation of Coherent Light," IEEE Student Journal, Vol. II, No. 5, pp. 18-23, (September, 1964).

4. I. P. Kaminow, "Microwave Modulation of the Electro-optic Effect in KH_2PO_4," Physical Review Letters, Vol. 6, No. 10, pp. 528-530, (May 15, 1961).

5. W. Niblack and E. Wolf, "Polarization Modulation and Demodulation of Light," Applied Optics, Vol. 3, No. 2, p. 277, (February, 1964).

6. C. F. Buhrer, L. R. Bloom, and D. H. Baird, "Electro-optic Light Modulation with Cubic Crystals," Applied Optics, Vol. 2, No. 8, pp. 839-846, (August, 1963).

7. Gordon M. Russel, Modulation and Coding in Information Systems, Englewood Cliffs, N. J., Prentice-Hall, 1962.

8. M. Schwartz, Information Transmission, Modulation, and Noise, New York, McGraw-Hill, 1959.

9. "Electro-optic Light Modulators: KDP, ADP, KD*P, and Supplementary Electronics," March, 1965, Baird-Atomic Inc., 33 University Road, Cambirdge, Massachusetts, 02138.

10. Frederick E. Terman, Electronic and Radio Engineering, New York, McGraw-Hill, 1955.

11. John J. Downing, Modulation Systems and Noise, Englewood Cliffs, N.J., Prentice-Hall, 1964.

12. Joseph F. Stephany, "Piezo-optic Resonances in Crystals of the Dihydrogen Phosphate Type," Journal of the Optical Society of America, Vol. 55, No. 2, p. 136, (February, 1965).

13. D. F. Holshouser, H. Von Foerster, and G. L. Clark, "Microwave Modulation of Light Using the Kerr Effect," Journal of the Optical Society of America, Vol. 51, No. 12, pp. 1360-1365, (December, 1961).

14. G. D. Boyd and H. Kogelnik, Bell Systems Technical Journal, Vol. 41, p. 1347, (1962).

15. "Single-frequency Laser Produced Without Loss of Power," IEEE Spectrum, Vol. 2, No. 9, p. 18, (September, 1965).